Materials Today • Volume xxx, Number xx • xxxx 2024

ELSEVIER

RESEARCH: Review

Inverse design of phononic meta-structured materials

Hao-Wen Dong [a,*], Chen Shen [c,*], Ze Liu [d], Sheng-Dong Zhao [e], Zhiwen Ren [a], Chen-Xu Liu [f], Xudong He [a], Steven A. Cummer [g], Yue-Sheng Wang [b,*], Daining Fang [a,h], Li Cheng [d]

[a] Institute of Advanced Structure Technology, Beijing Institute of Technology, Beijing 100081, China
[b] Department of Mechanics, School of Mechanical Engineering, Tianjin University, Tianjin 300350, China
[c] Department of Mechanical Engineering, Rowan University, Glassboro, NJ 08028, USA
[d] Department of Mechanical Engineering, The Hong Kong Polytechnic University, Hong Kong, China
[e] School of Mathematics and Statistics, Qingdao University, Qingdao 266071, China
[f] Department of Engineering Mechanics, School of Aerospace, Tsinghua University, Beijing 100084, China
[g] Department of Electrical and Computer Engineering, Duke University, Durham, NC 27708, USA
[h] College of Engineering, Peking University, Beijing 100871, China

Flexible manipulation of elastic and acoustic waves through phononic meta-structured materials (PMSMs) has attracted a lot of attention in the last three decades and shows a bright future for potential applications in many fields. Conventional engineering design methods for PMSMs rely on changing the material composition and empirical structural configurations, which often result in limited performance due to the limited design space. Recent advances in the fields of additive manufacturing, optimization, and artificial intelligence have given rise to a plethora of creative meta-structured materials that offer superior functionality on demand. In this Review, we provide an overview of inverse design of phononic crystals, phononic-crystal devices, phononic metamaterials, phononic-metamaterial devices, phononic metasurfaces, and phononic topological insulators. We first introduce fundamental wave quantities including dispersion relations, scattering characterizations, and dynamic effective parameters, and then discuss how these wave quantities can be leveraged for systematic inverse design of PMSMs to achieve a variety of customized phononic functionalities with highly customizable full-wave responses, intrinsic physical parameters, and hybrid local–global responses. Furthermore, we show representative applications of some inverse-designed PMSMs and look at future directions. We outline the concept of phononic structures genome engineering (PSGE) through key developments in PMSM inverse design. Finally, we discuss the new possibilities that PSGE brings to wave engineering.

Keywords: Elastic/Acoustic waves; Meta-structured materials; Topology optimization; Machine learning; Phononic structures genome engineering

Introduction

Elastic and acoustic wave manipulation

Sound and vibration are the result of wave propagation in an elastic medium and are ubiquitous in everyday life. Depending

* Corresponding authors.
E-mail addresses: Dong, H.-W. (hwdong@bit.edu.cn), Shen, C. (shenc@rowan.edu), Wang, Y.-S. (yswang@tju.edu.cn).

Please cite this article in press as: H.-W. Dong et al., Materials Today, (2024), https://doi.org/10.1016/j.mattod.2024.09.012

on the medium of propagation, problems are generally divided into two categories: acoustic waves in fluids and elastic waves in solids. These waves carry energy and useful information and have a wide range of applications. As a prime example, most animals use vocalized sounds to communicate within the same species and even with other species. Controlling sound and vibration has played an important role in human history. For instance, resonant structures have long been used in different scenarios, exemplified by the design of musical instruments, especially string and wind instruments. At the same time, the adverse effects of sound and vibration on the quality of human life and on the competitiveness of manufactured goods and engineering structures have triggered persistent and intensive research efforts. To achieve the ultimate goal of flexible manipulation/mitigation of sound and vibration, we need a fundamental understanding of the underlying physics that dictates wave propagation and sound-matter interactions, as well as effective approaches for designing structures or materials with specific functionality. Over the past few decades, this long-term quest has led to the emergence of a new class of engineered materials that greatly extend the wave manipulation capability. They typically constitute subwavelength scatterers that display extraordinary properties beyond those of conventional materials, and are coined as phononic meta-structured materials (PMSMs), representing a class of artificial functional material with microstructures or hierarchical structures consisting of functional morphological building blocks distributed in a specific pattern. By designing the topology and the hierarchical ordering, carefully crafted PMSMs allow for flexible shaping of elastic/acoustic properties that are unattainable in nature materials. For the remainder of this Review, the definition of PMSMs covers the full range of phononic crystals [1,2], phoxonic crystals [3,4], phononic-crystal devices [5–7], phononic topological insulators [8–10], acoustic/elastic metamaterials [11,12], acoustic/elastic-metamaterial devices [13,14], acoustic/elastic metasurfaces [15,16], as well as other derived devices for of elastic/acoustic manipulation and diverse applications [17–28] (Fig. 1).

Phononic meta-structured materials

The history of PMSMs can be traced back to the 1970s, when researchers began investigating the forbidden frequency bands in which sound waves are unable to propagate in periodic structures [1,29–32]. These periodic structures (i.e., the earliest phononic crystals named after periodic elastic composites [32–34] represented the first examples of PMSMs and led the wave of development of PMSMs in the following decades. Starting in the 2000s, efforts were made to reduce the footprint of phononic crystals to subwavelength scales through embracing enhanced wave-matter interactions [11,35]. This type of PMSMs, known as acoustic metamaterials, employ locally resonant elements as building blocks, which collectively exhibit exotic effective properties not found in nature. In the last decade, acoustic metasurfaces, a two-dimensional (2D) equivalent of acoustic metamaterials, have emerged for versatile control of sound waves with ultrathin profiles. Acoustic metasurfaces have further expanded the capacity of PMSMs for sound wave manipulation [15,36,37]. Together, these PMSMs have revolutionized strategies for achieving sound and vibration control in unprecedented ways. They have enabled unparalleled flexibilities in a plethora of applications such as imaging, sound absorption, acoustic communications, and so on [35,37–43].

Intuitive design of phononic meta-structured materials

The development of PMSMs relies on the ability to design artificial structures that exhibit specific properties or lead to specific wave-matter interaction patterns. While PMSMs offer tremendous possibilities for the manipulation of sound and vibration energy, their design is not a trivial task. Conventional design of PMSMs rely on intuitive concepts and structures with simple geometries, e.g., membrane- and plate-type metamaterials as building blocks for sound absorbing metamaterials due to their ability to provide negative effective densities [36,44,45]. On the other hand, phononic crystals made of circular or rectangular scatterers have been mainly used as bandgap materials for filtering or sensing applications [46–50]. Despite their simple configurations and useful features, they suffer from the limited space for design freedom and achievable features. Facing the growing demand and expanded functionality, these conventional design approaches are not able to cope with some of the new challenges in the development of PMSMs, especially in terms of satisfying large-scale use and user-demanded features. In recent years, along with the advances in numerical simulations and optimization methods, inverse design techniques and data-driven approaches have been widely applied to PMSM design [51–58].

Outline of the paper

In this Review, we summarize the latest advances and challenges in PMSMs. We first introduce the basic approaches to inverse design of PMSMs, namely topology optimization (ToP), machine learning, and other optimization approaches. We also highlight novel features and functionalities of PMSMs realized through various design techniques. We then provide an overview of inverse-designed PMSMs and their associated customized functionalities, which cover phononic crystals, metamaterials as well as topological insulators. We extend the discussion of inversely designed PMSMs to the concept of phononic structures genome engineering (PSGE) and outline its potential impact on the overall structural design and synthesis. Finally, we conclude this Review with an outlook and a fresh perspective. The limitations of current approaches and emerging directions are also discussed.

Inverse-design methodology for PMSMs

The properties of PMSMs mainly depend on their constitutive microstructures, which contain specific topology and hierarchical ordering [35,38,41,59–61]. Therefore, designing hierarchical structures in a systematic, intelligent, and modular manner has always been a core task in the field of PMSMs. To overcome the limitations of manual and empirical design, promising attempts were made to inversely design the topology of component microstructures [62] and the microstructural sequence [63,64] for on-demanded realization of extreme physical properties, and exotic phenomena [54] or functionalities [52]. Theoretically, the core of inverse designing PMSMs lies in constructing suitable optimization models, regardless of topology design of topology [51,54,55] or the determination of geometric parameters [53,65,66]. Depending on the specific requirements of PMSMs,

Please cite this article in press as: H.-W. Dong et al., Materials Today, (2024), https://doi.org/10.1016/j.mattod.2024.09.012

FIG. 1

Phononic meta-structured materials (PMSMs) and potential applications. Reproduced with permission from Refs. [1–4,8,10–28,38].

such as multi-functional [67], large-scale [53], or high-throughput integrated design-manufacturing [68], the models need to be tailored by constructing objective functions and constraints, while being able to accurately describe the desired wave characteristics, incorporate the physical mechanisms of wave control, avoid numerical mutations, and exhibit robustness to perturbations. Undoubtedly, the inverse design of PMSMs should be an indispensable bridge between the proof-of-concept demonstration and practical application of functionalized PMSMs.

This section will discuss the basic characterization quantities of wave propagation used for inverse design, as well as three representative types of inverse-design methodologies for PMSMs for obtaining target elastic or acoustic wave motions.

Fundamental wave quantities for inverse design

Obtaining customized elastic or acoustic wave functionality requires careful design of the desired physical wave quantities. Three typical quantities are usually used, namely the dispersion relation (ω-k), the scattering characterization quantity and dynamic effective parameter.

Dispersion relations

As one of the most fundamental ways to characterize wave propagation, dispersion relation describes the interdependence between the time-domain and spatial-domain states and is expressed by a function involving frequency and wave vector (number). Many other characterization quantities of waves can then be derived from the dispersion relation, such as the equal-frequency contours (surfaces), group velocity, phase velocity, density of state, etc. In particular, wave modes can be identified from the dispersion relation, which is extremely important for wave characterization. In contract to the commonly-used real-part dispersion relation, the complex dispersion relation can quantitatively characterize the wave dissipation, especially for viscoelastic media. When a bandgap is created, elastic and acoustic waves decay exponentially. Optimizing the relative bandgap widths can entail broadband vibration isolation [51]. Designing directional bandgaps can enable unidirectional high-transmission in waveguides [69,70]. Using weighted objective function, phononic multiple wave filters can also be realized [71]. If a point defect is introduced in the PMSMs, a high-quality cavity can be inverse-engineered [67,72]. Such customized high-Q phononic cavities can also be achieved by simul-

Please cite this article in press as: H.-W. Dong et al., Materials Today, (2024), https://doi.org/10.1016/j.mattod.2024.09.012

taneously tuning the eigenmode and dispersion relation [73]. The dispersion relation can be further extended to incorporate strong optomechanical coupling through multi-objective optimization and meticulous tuning of photonic and phononic modes [67]. Recently, non-local effects have been taken into account to demonstrate Roton-like dispersion relation [74], which greatly expanded wave control capabilities. On the other hand, equal-frequency contours allow for the control of the scattering of the incident waves when interacting with PMSMs. For example, highly anisotropic self-collimation [75], negative refraction [76], and directional transmission [77] can be realized by optimizing the equal-frequency contours or the group velocities. In addition, phononic topological insulators can be obtained by designing local state densities for desired Dirac cones with different degeneracies [78,79].

Scattering characterization quantities

Scattering problems including reflection, refraction, and diffraction commonly use quantities such as wave transmission, absorption, and reflection coefficients as well as the scattering cross-section. The transmission coefficient describes the transmitted wave flux or energy power with respect to the incident counterparts, and is an important quantifying parameter in achieving highly efficient refractive waves [80,81] or in superlensing [82]. On the contrary, the reflection coefficient needs to be minimized, often over a specific frequency range, for sound absorber design [81]. The phase and amplitude of scattered waves can also be leveraged in designing PMSMs. For example, systematically optimizing the phase gradient of phononic metasurfaces allows for broadband wavefront manipulation [52]. With a multi-bit coding distribution, broadband diffused reflection or transmission can be further realized [83]. Incorporating both phase and amplitude modulation contribute to high-resolution acoustic holograms [53] and underwater particle manipulation [16]. For the abnormal reflection of elastic waves, the customized mode conversion between the interfaces can be leveraged to achieve a single wave motion [84], conductive to applications like underwater acoustic stealth, medical ultrasound and nondestructive testing. Such customized wave mode conversion can be exploited for both underwater sound absorption/insulation when wave polarization is considered [85]. Recently, asymmetric topologies of some PMSMs have been proposed to induce the Willis coupling effect [86], which shows great potential for ultrasound testing.

Dynamic effective parameters

Wave motion of phononic metamaterials can be described by their homogenized dynamic effective parameters [87–89], including effective mass density, refraction index, bulk modulus, longitudinal modulus and shear modulus. Quantitative design of these parameters can produce PMSMs with tailored wave propagation properties and trajectories. For example, one needs to create low-frequency broadband negative effective mass densities when designing a low-frequency vibration isolator or absorber [82]. In particular, when the effective mass densities show strong anisotropy, a metamaterial exhibits a hyperbolic dispersion feature which can be used to generate high-efficiency directional wave propagation and hyperlens [90–93]. Similarly, negative effective bulk modulus is critical for constructing microstructures for sound absorbers or acoustic cloaking [94,95], i.e., periodic resonant cavities can be optimized for limit-pushing low-frequency air absorption/acoustic isolation. If both negative mass density and negative modulus are supported, metamaterials can acquire negative group velocities in a certain band, thus enabling negative refraction and subwavelength imaging [96–98] as well as 2D/3D superlens [54,98,99]. Notably, a single negative metamaterial can also support a negative refractive index if multiple scattering is introduced [100]. A near-zero mass density or refractive index can lead to wave tunneling against the effect of defect-based scattering [54]. For elastic metamaterials, negative effective moment of inertia can be captured and verified when a fin-like resonant element is embedded [101]. In addition to negative, zero or infinite values of the effective parameters, a suitable combination of the effective moduli can further enable extreme wave features. For example, if the shear modulus is suppressed while keeping the coupling modulus close to the longitudinal modulus, pentamode metamaterials can be obtained to behave like water [102–104]. Balancing the longitudinal, shear, and coupling moduli allows anisotropic elastic metamaterials to achieve significant longitudinal–transverse mode transitions [84,85,105,106], which is conducive to ultrasonic imaging, nondestructive testing and underwater stealth, etc.

In summary, basic wave quantities depend on the required wave functionality. As shown in Fig. 2, based on suitable wave quantities in Fig. 2a–c, new PMSMs can be inversely designed on-demand through building proper mathematical model with physical single-objective/multi-objective optimization functions in Fig. 2d and e with constraints through the corresponding optimization or machine-learning algorithms in Fig. 2f–h. Notably, to date, the fundamental wave quantities involved in most existing studies on the inverse design of PMSMs belong to the low-order linear elastic system only. This can pose a challenge when non-Hermiticity [107–109] is introduced in wave problems, and thus new wave quantities should be developed to capture their effects. The inverse design of a PMSM can lead to breakthroughs at three different levels, namely, brand-new topological features

FIG. 2

Schematics of inverse-design methodology for constructing PMSMs. (a–c) Typical full-wave responses, intrinsic parameters, and local–global responses that are usually adopted in optimization. (d–e) Two classic optimization problems in the whole field. Multi-objective optimization usually characterizes a multiple-functional PMSM or a PMSM in the multi-physics field. (f–h) Three mainstream methods for solving inverse problems of elastic/acoustic waves. Gradient optimization is suitable for differentiable and derivable problems. Some complex non-convex problems can be settled by the non-gradient optimization. For the fast/on-line design, the machine-learning models are good choices because of their strong nonlinear fitting abilities. (i) A multi-hierarchical PMSM with elaborate-designed topologies at three levels/scales. Diversiform square-symmetry, chiral, orthogonal-symmetry, and bilateral-symmetry structures using the solid–solid/solid-air materials are generated by one of the inverse-design approaches in (h).

Please cite this article in press as: H.-W. Dong et al., Materials Today, (2024), https://doi.org/10.1016/j.mattod.2024.09.012

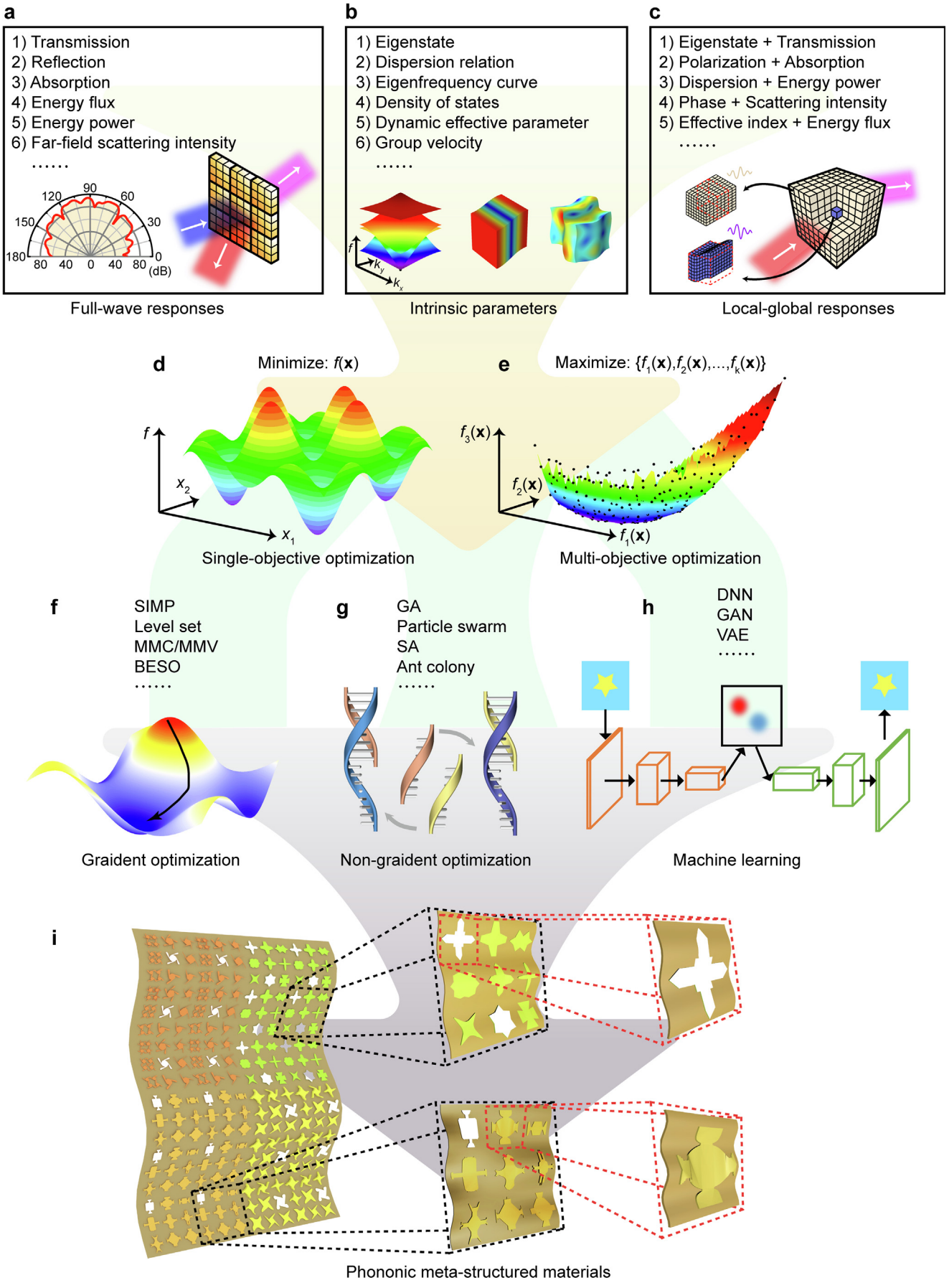

Please cite this article in press as: H.-W. Dong et al., Materials Today, (2024), https://doi.org/10.1016/j.mattod.2024.09.012

(Fig. 2i), near-optimal or optimal wave performance/functionality, and novel physical mechanisms to simplify the architecture of the model for enhanced effectiveness. In other words, a more rational inverse-design model incorporating more physical essences should be built for customizing PMSMs with signature topological features.

Topology optimization (ToP)

As a representative inverse-design method, ToP [110] has been widely used in the field of engineering [111–117]. Essentially, ToP is a numerical method that can simultaneously handle changes in the structural geometry and physical properties [111]. The importance of ToP in structural design lies in transforming the traditional empirical design method of trial and error into an automatic optimization paradigm based on a mathematical model. For the systematic design of PMSMs, the mathematic modelling of ToP (including the objective function, constraints, and design variables, etc) is vital because appropriate parameters can judiciously guide the optimization to find the right searching direction in the feasible solution space. The modelling can be conducted through full-wave responses, intrinsic physical parameters, and hybrid local–global responses according to the type of physical quantities adopted. As such, ToP has been successfully implemented in periodic [54,55], gradient [52], hierarchical [118], and multiscale [119–121] PMSMs.

ToP with full-wave responses

From the perspective of whole macrostructure, ToP of PMSMs essentially lies in the use of innovative structures to control wave energy distribution [80]. Given a pre-defined full-wave response, e.g., transmission/reflection efficiency or propagation path of waves, ToP shapes the PMSMs to arrive at the proper structure. To this end, a physical model needs to be built to predict the main propagation characteristics [80], which subsequently determines effective means to guide the propagation mode of energy flux [80,81], etc. Special attention needs to be paid by choosing the suitable extracting location of full-wave responses so that an optimized macrostructure can be effectively generated [122]. When the coupling between multiple elastic wave modes is involved, the optimization model should restrict the coupling with the prescribed wave efficiency or propagation path [81]. For underwater applications [39], additional effects caused by the viscous loss of the medium and hydrostatic pressure need to be considered.

For example, to construct a phononic topological insulator [123], traditional intuitive design was usually based on bottom-up band engineering by exploring different eigenstates. As illustrated in Fig. 3a–c, to consider the coupling effect of a finite-size model and seek the optimal design, the interpolation of material parameters using the density-based approach was used during optimization for the hexagonal design domain consisting of two kinds of unit cells with C3v symmetry. Then a top-down ToP formulation based on the acoustic intensities in different regions was established. Introducing an initial structure with a trivial bandgap, maximizing the difference of acoustic energy intensity between three ports and alternate ports can produce a pseudospin acoustic topological insulator, resulting in a high-transmission beam splitter with an operational bandwidth of ≈12.5 %.

Similarly, as shown in Fig. 3d–f, a full-wave response is conductive to realizing high-efficiency negative refraction [80,124]. For a design domain containing periodic orthosymmetric microstructures in a square lattice, the material parameters of solid and vacuum were interpolated based on the density-based method. A ToP formulation can be built by combining the min/-max problem on wave energy with a volume constraint. After introducing an initial structure with circular scatterers, minimizing the standard deviation between the target beam energy and the obtained energy directly gives rise to layout of the novel scatterers distributed in the air. As a result, the method can expediently create the high-efficiency (transmittance>80 %) negative-refraction beam under single- or multiple-incident beams within prescribed incidence angles or refractive indices.

ToP has many advantages such as simple/clear objective function, high-efficiency in waveform control, compatibility, and strong universality, etc. However, it also has disadvantages, i.e., the topology is complex, time-consuming, lack of physical mechanisms, and high processing cost. For multi-physics coupling problems [67,125–127], the topology-optimization methodology relies heavily on a high-efficiency forward computing method to obtain effective full-wave responses [123]. The large number of design variables [46,128,129] can also pose a significant challenge to optimizing, especially for non-convex problems. In particular, if the problem comprises a strong boundary coupling effect [46,51,73], the optimized PMSMs are usually case-by-case and difficult to extend to other models with specific boundaries or dimensions.

ToP with intrinsic physical parameters

From the microstructural point of view, the essence of ToP for PMSMs lies in the enhancement of the coupling between elastic/acoustic waves and the microstructure by means of the specialized microscopic topology. Based on the intrinsic physical parameters of a microstructure (e.g., dynamic effective mass density [96], effective modulus [94], dispersion relation [130], eigenfrequency curves [10], density of states [131], phase and amplitude [37,132,133], etc.), ToP can create microstructures with different topological configurations to customize dynamic intrinsic properties. These intrinsic physical parameters will then produce macroscopic effects manifested as various transmission, reflection, scattering, or diffraction effects. To implement this approach, a suitable physical model incorporating intrinsic parameters is required to elucidate the main patterns of variation of intrinsic parameters, the underlying physical mechanism, and the application ranges of effective medium theory. In most cases, the optimization model must take into account the effect of topological symmetries [134–136] on the intrinsic parameters to accelerate convergence and highlight the physical features [54]. To deal with special scenarios, other features may also be included in the model. Examples include multi-objective functions or multi-constraints for multi-physics fields [67], special energy constraints regarding the motion and eigenmodes when complex motions of microstructures such as boundary rotations and asymmetric twists are induced as well as neighboring and neighboring-beyond nonlocal effects [133,137]. In particular,

Please cite this article in press as: H.-W. Dong et al., Materials Today, (2024), https://doi.org/10.1016/j.mattod.2024.09.012

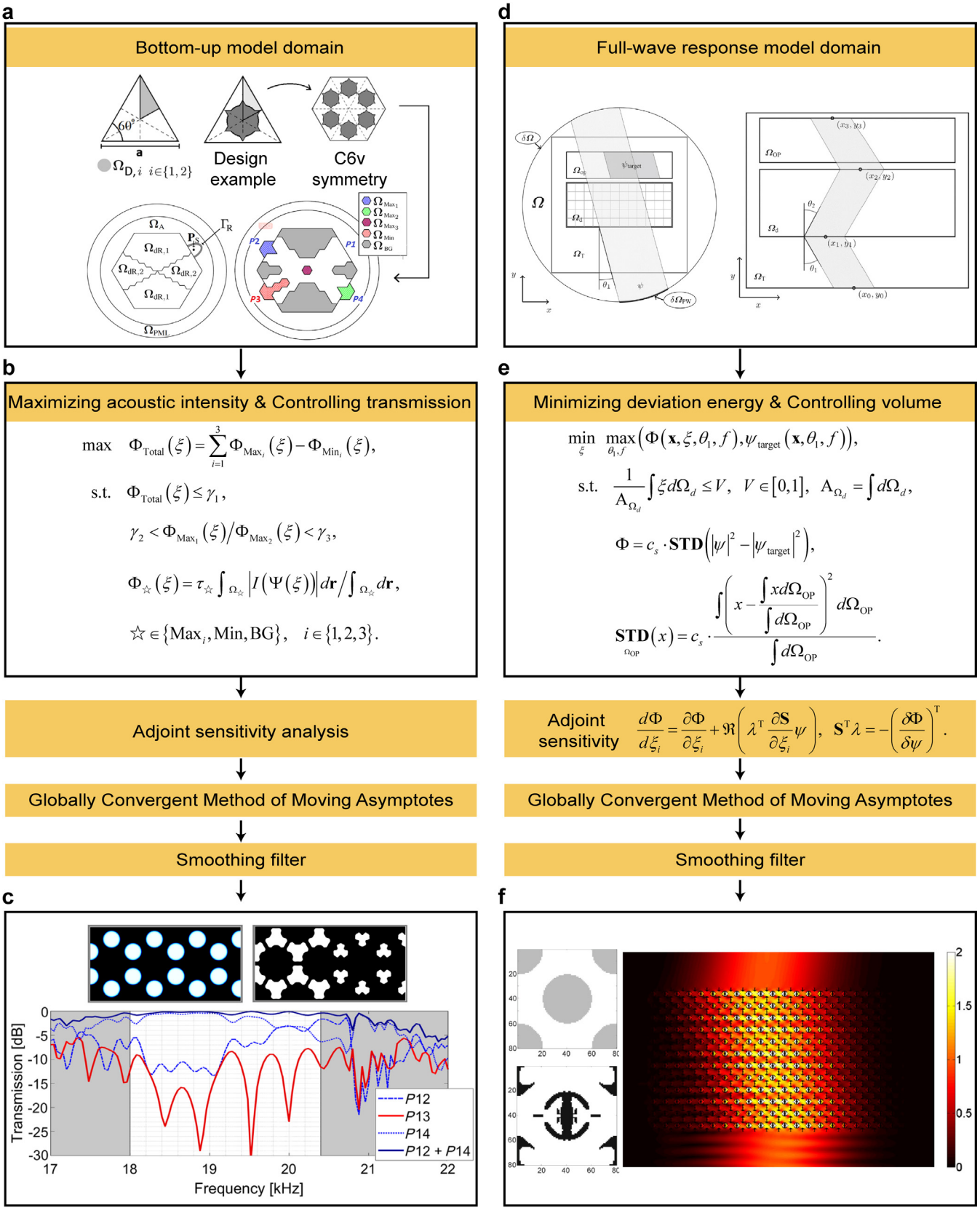

FIG. 3

ToP of acoustic pseudospin-dependent topological insulators and acoustic hyperbolic metamaterials using a top-down approach based on density-based optimization. (a–c) Method of constructing a broadband acoustic topological insulator for broadband topological transmission. Permission adopted from Ref. [55]. (d–f) Strategy for designing the metamaterial-enabled acoustic negative refraction under an incoming wave with an arbitrary angle of incidence. Permission adopted from Ref. [80].

Please cite this article in press as: H.-W. Dong et al., Materials Today, (2024), https://doi.org/10.1016/j.mattod.2024.09.012

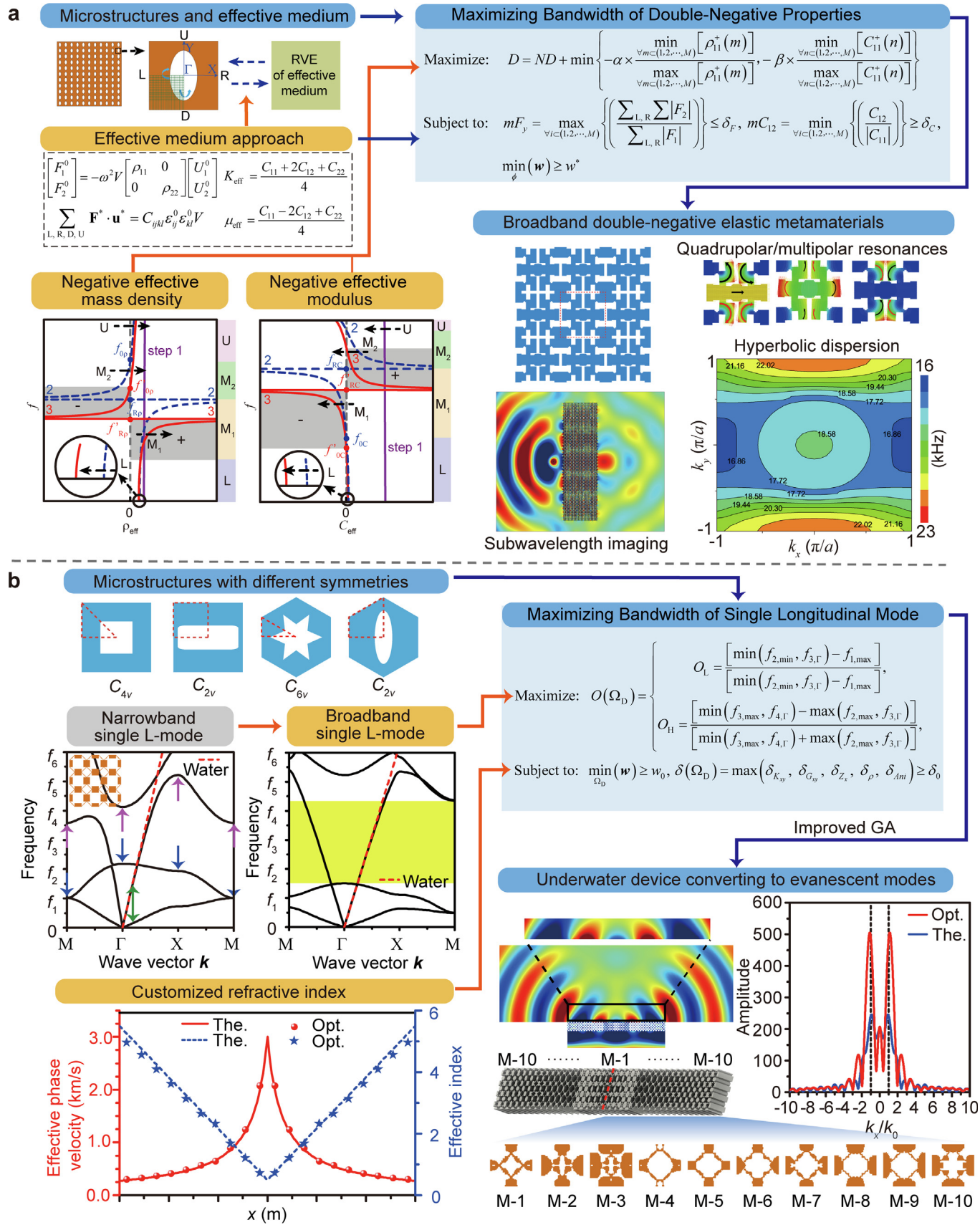

Please cite this article in press as: H.-W. Dong et al., Materials Today, (2024), https://doi.org/10.1016/j.mattod.2024.09.012

when soft polymer materials or smart materials are utilized for microstructures, the non-linear mechanics need to be introduced into the optimization model [137].

For example, double-negative elastic metamaterials have been constructed in the targeted broadband range using an ingenious combination of positive/negative effective mass density and elastic modulus [54]. As illustrated in Fig. 4a, the subwavelength-scale microstructures composed of porous solids represent the design domain. Due to the complexity of the dynamic effective features, it is important to explore the regularity of evolution of the effective mass density and elastic modulus under the mechanism of resonances. Then positive/negative effective mass density and elastic modulus at different sampling frequencies were embedded into the ToP formulation. Besides, three specific constraints were introduced to ensure that the microstructure satisfies local vibration requirement and manufacturing feasibility. Using the improved GA, the maximization of the difference between the maximum positive value and the minimal positive one can lead to the double-negative effective parameters. Ultimately, this design approach can create distinctive broadband double-negative elastic metamaterials induced by novel quadrupolar or multipolar resonances, supporting subwavelength imaging of longitudinal waves and perfect cloaking of longitudinal or transverse waves.

For constructing microstructures with specific wave modes in underwater environments, an elaborate ToP strategy was needed to regulate the relationship between all positive effective elastic moduli [138]. As displayed in Fig. 4b, four types of microstructures with different symmetries in the square and triangle lattices were considered. To reach a single longitudinal wave mode in the low-frequency broadband range, two design strategies were developed to optimize the microstructures. That is, to widen the frequency range between the first- and second-order bands or to broaden the frequency range between the second- and third-order bands while satisfying the requirements of the pentamode feature. These two approaches can be uniformly described as optimizing the longitudinal-mode dispersion curves under the constraints of multiple pentamode feature parameters and minimal geometrical dimensions. The approach based on improved GA can inversely design multiple new pentamode metamaterials, i.e., free isotropic pentamode metamaterials, isotropic, anisotropic pentamode metamaterials with impedance matching, anisotropic pentamode metamaterials with impedance matching and prescribed anisotropy, etc. Using the gradient distribution, a pentamode metasurface was constructed to convert an incident plane wave into an evanescent wave for underwater acoustic insulation.

As shown in Fig. 5, ToP to realize passive ultrabroadband and frequency-independent acoustic metasurface requires consideration of complex dispersion characteristics [52]. An analysis of macroscopic and microcosmic dispersion features revealed that the key to produce achromatic properties was to satisfy the requirements of specific effective refractive index, relative group delays, and relative group delay dispersions. For the design domain constituting metasurface elements, a bottom-up ToP formulation was established based on the phase, efficiency, and dispersions. A series of acoustic metasurface elements were designed to capture the customized linear/nonlinear dispersions. Then a novel acoustic metasurface was constructed through substantialization and assembly. As a result, broadband achromatic acoustic beam engineering was realized systematically, including directional transmission, energy focusing, and ultrasound particle levitation. Notably, the studies revealed the underlying mechanism underpinning the broadband achromatic nature, i.e., the synthesis of integrated internal resonances, bi-anisotropy, and multiple scattering.

Compared with ToP based on full-wave responses, ToP involving intrinsic parameters has the advantages of low computational complexity and physical determinism. However, it also faces several challenges such as non-differentiable/non-derivable/discontinuous/mutational objective function, multiplicity of solutions, and poor universality. Moreover, if the optimization targets are complex wave modes or strongly dispersive, this topology-optimization method has demanding requirements on the universal dynamic effective medium theory. In general, this methodology can be treated as a local design method that cannot guarantee the consistency of local physical features of microstructures and wave functionality, e.g., the high-order diffraction waves [15,65,139] will be derived for the acoustic gradient metasurfaces.

ToP with hybrid local–global responses

Unlike the independent design of full-wave responses or intrinsic parameters, one usually needs to tailor the global full-wave and local intrinsic parameters synchronously for complex physical systems or models. This is particularly true for multi-hierarchical PMSMs which bear complex topology at the macroscopic scale and periodic microstructures at the microscopic scale. Inspired by biological materials, multi-hierarchical structures [119] have been widely used for improving and optimizing the physical properties of composite material structures that have specific structures at multiple scales and ordering modes. For acoustic and elastic waves, the multi-scale ToP of a multi-hierarchical structure should be based on the construction of multi-scale collaborative optimization models that synthesize the intrinsic physical parameters of the microstructures and the full-wave responses of the macrostructures in order to capture

FIG. 4

ToP of double-negative elastic and pentamode metamaterials using a bottom-up approach based on heuristic optimization. (a) Anisotropic elastic metamaterials with broadband double negativity designed by improved genetic algorithm (GA) considering the resonance mechanism, boundary's deformation, and coupling modulus. Dispersions along the *x*- and *y*-directions are dominated by double-negative and hyperbolic features, respectively. Reproduced with permission from Ref. [54]. (b) Customized square- and triangle-latticed pentamode metamaterials for broadband longitudinal wave manipulation designed by a dispersion-engineered optimization which incorporates the prescribed effective density, anisotropy, impedance, and pentamode feature simultaneously. Reproduced with permission from Ref. [138].

Please cite this article in press as: H.-W. Dong et al., Materials Today, (2024), https://doi.org/10.1016/j.mattod.2024.09.012

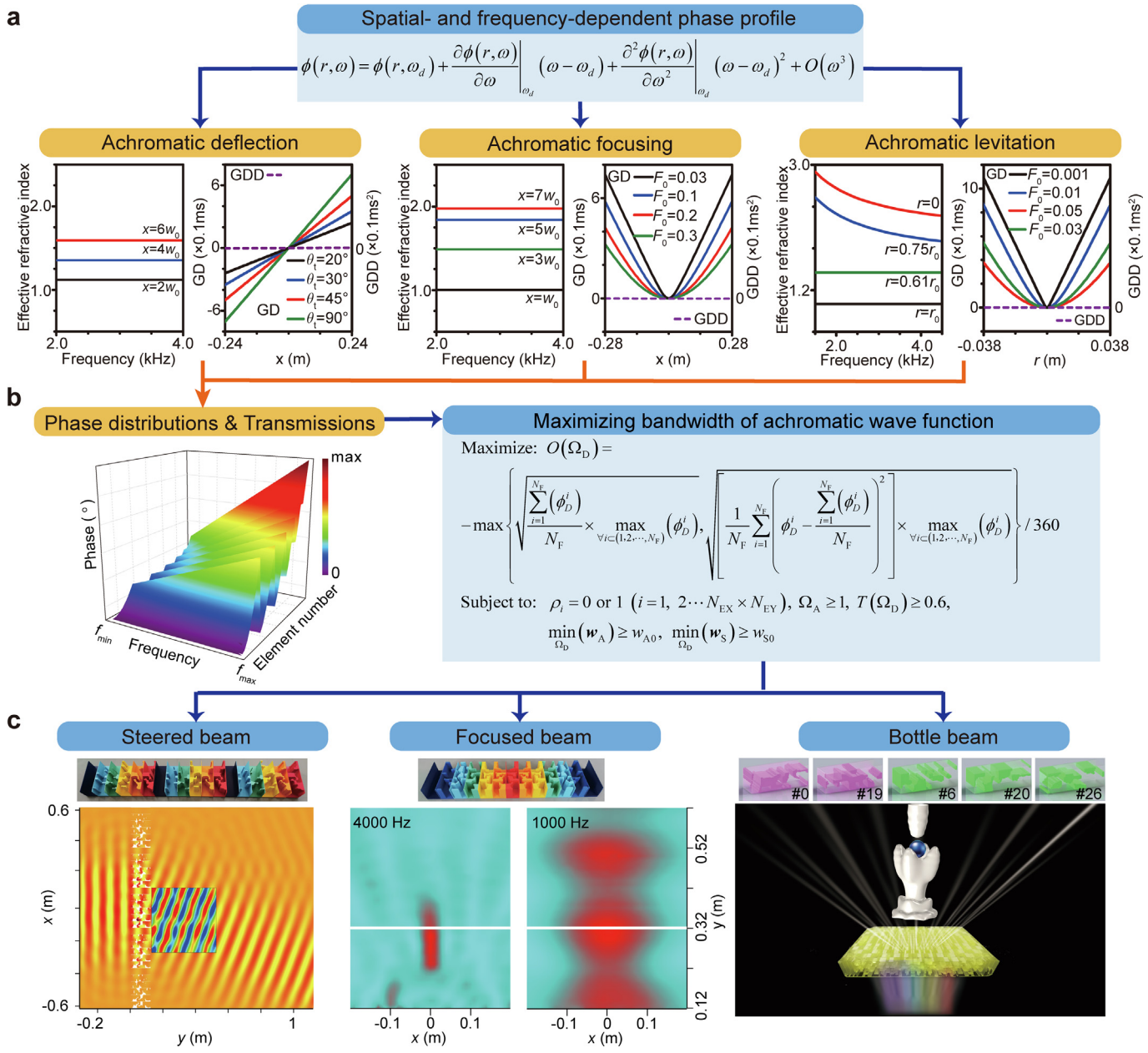

FIG. 5

ToP of achromatic acoustic metasurfaces with customized dispersions for ultrabroadband beam engineering. (a) Macroscopic and microscopic dispersions for achromatic deflection, focusing, and levitation. (b) A heuristic bottom-up ToP of a metasurface for customized dispersions on mand and representative optimized elements. (c) Ultra-broadband acoustic functionalities originated from steered, focused and bottle beams with achromatic features using three designed metasurfaces consisting of different anisotropic and asymmetric elements. Reproduced with permission from Ref. [52].

the physical responses of both. Combing the static and dynamic effective medium theories [140], the optimization model can generate the density of every sub-region of the macrostructure as well as effective material parameters that are realized by the corresponding microstructure topology. Subsequent assembly of all optimized microstructures into the macrostructure according to the optimized ordering pattern can lead to a breakthrough in extreme mechanical, physical, and multi-physical functionalities. If the cost for calculating the entire structural response is not high, it is usually more suitable to use ordinal multi-scale ToP [119], i.e., to obtain the material distribution based on the macrostructural wave responses, and then to design the microstructural topology according to the target effective material parameters. To reduce the computation cost, it is a common practice to employ concurrent multi-scale ToP [141,142], i.e., to simultaneously optimize both the microstructural distribution at the macroscale and the microstructural topology at the microscale. The salient merit of this topology-optimization methodology is that it accelerates the optimization of high-resolution structures [143], while greatly reducing the commuting cost. As a result, the wave properties/functionalities of the optimized PMSMs are expected to be close to the theoretical limit. However, the method poses practical challenges for the manufacturability of the structures. Obviously, the topological complexity

Please cite this article in press as: H.-W. Dong et al., Materials Today, (2024), https://doi.org/10.1016/j.mattod.2024.09.012

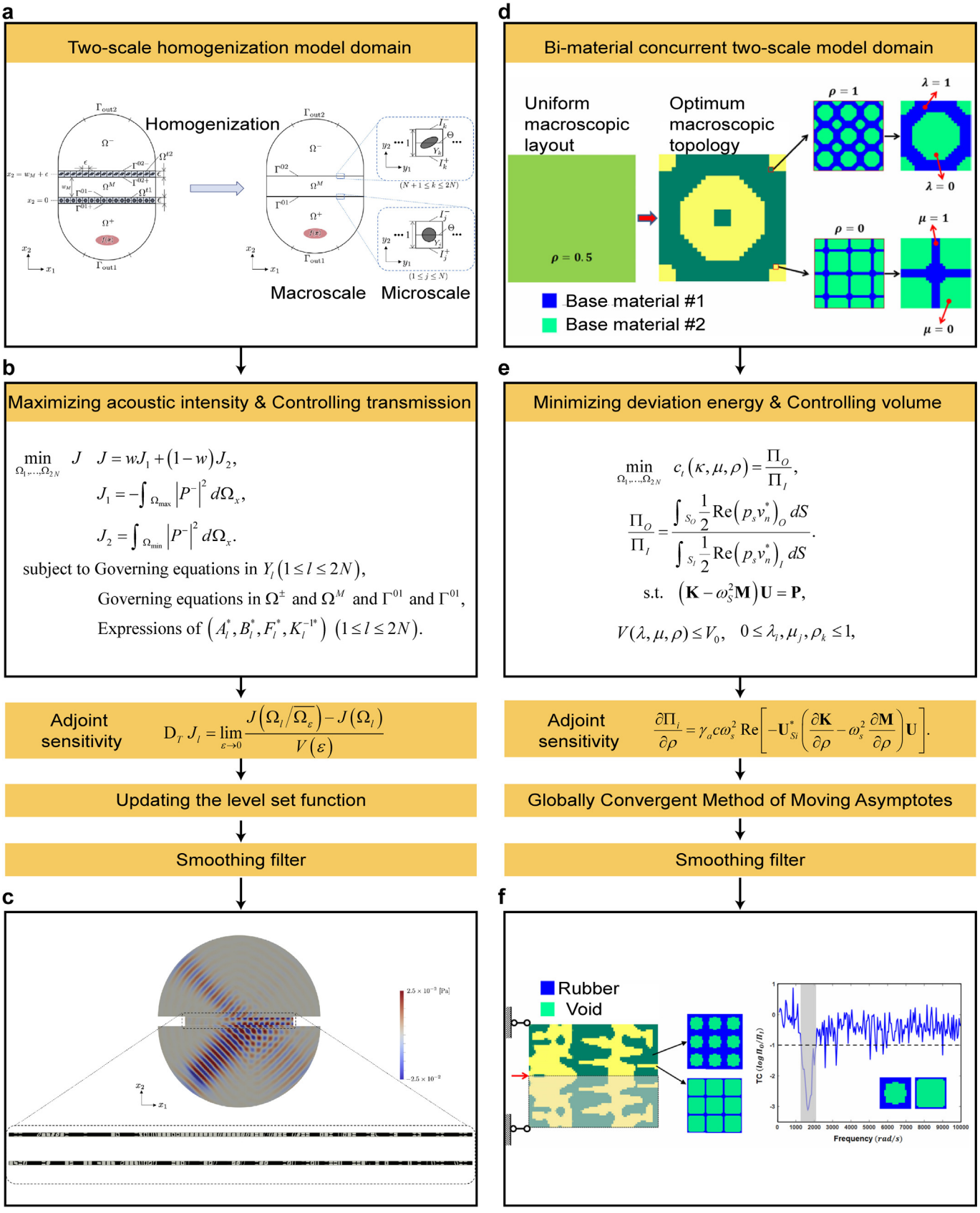

FIG. 6

Two-scale ToP of a graded acoustic metasurface and a vibro-acoustic phononic-crystal structure. (a–c) Graded acoustic metasurface with two layers designed by the level-set-based ToP using two-scale homogenization. Reproduced with permission from Ref. [146]. (d–f) Two-phase phononic-like structure designed by a concurrent two-scale ToP based on the SIMP approach. Reproduced with permission from Ref. [121].

Please cite this article in press as: H.-W. Dong et al., Materials Today, (2024), https://doi.org/10.1016/j.mattod.2024.09.012

[144,145] should be introduced in optimization model to explore the simpler microstructures and macrostructures that require lower processing requirements.

To construct negatively reflective acoustic metasurfaces with hybrid local–global responses, the key lies in how to felicitously introduce the non-local effects to maximize the design space [146]. As displayed in Fig. 6a–c, simultaneous consideration of both macroscopic acoustic wave efficiency and microscopic topology is an ideal design strategy to introduce non-local features. Considering material distributions of all microstructures as design variables, a ToP was formulated by combining a two-scale homogenization with SIMP. Each layer consisting of microstructures can be homogenized into an interface with non-local transmission conditions. The homogenized two-layer model can be used to characterize the acoustic full-wave response. Using a level-set optimization approach that simultaneously maximizes the refracted wave energy in the target region and minimizes the refracted wave energy in other regions, a bilayer acoustic metasurface that supports a prescribed negative refraction angle can be efficiently generated.

To further expand the space of phononic crystals, a feasible strategy is to integrate the topology of unit cells and macroscopic distribution in the ToP process [121]. As shown in Fig. 6d–f, for a composite structure comprising two types of microstructures, the effective elasticity tensor and the effective mass density can be evaluated based on the bi-material SIMP model. By minimizing the sound transmission coefficient, the optimization model allows the design of macroscopic structures assembled from two different phononic crystal unit cells for elastic wave attenuation and acoustic suppression within the target frequency range.

Machine learning

Machine learning is a powerful artificial intelligence technology, which leads to many breakthroughs in all aspects of life, such as ChatGPT [147], automatic driving [148], medical diagnosis [149], protein structure prediction [150], signal and image processing [151], and so on. In general, machine learning models are composite functions and can simulate or approximate arbitrary mapping laws. They can be trained with data or under certain constraints to learn the nature of physical laws and solve corresponding problems. In recent years, there has been a significant increase in research on machine learning-assisted inverse design of PMSMs [53,152–155].

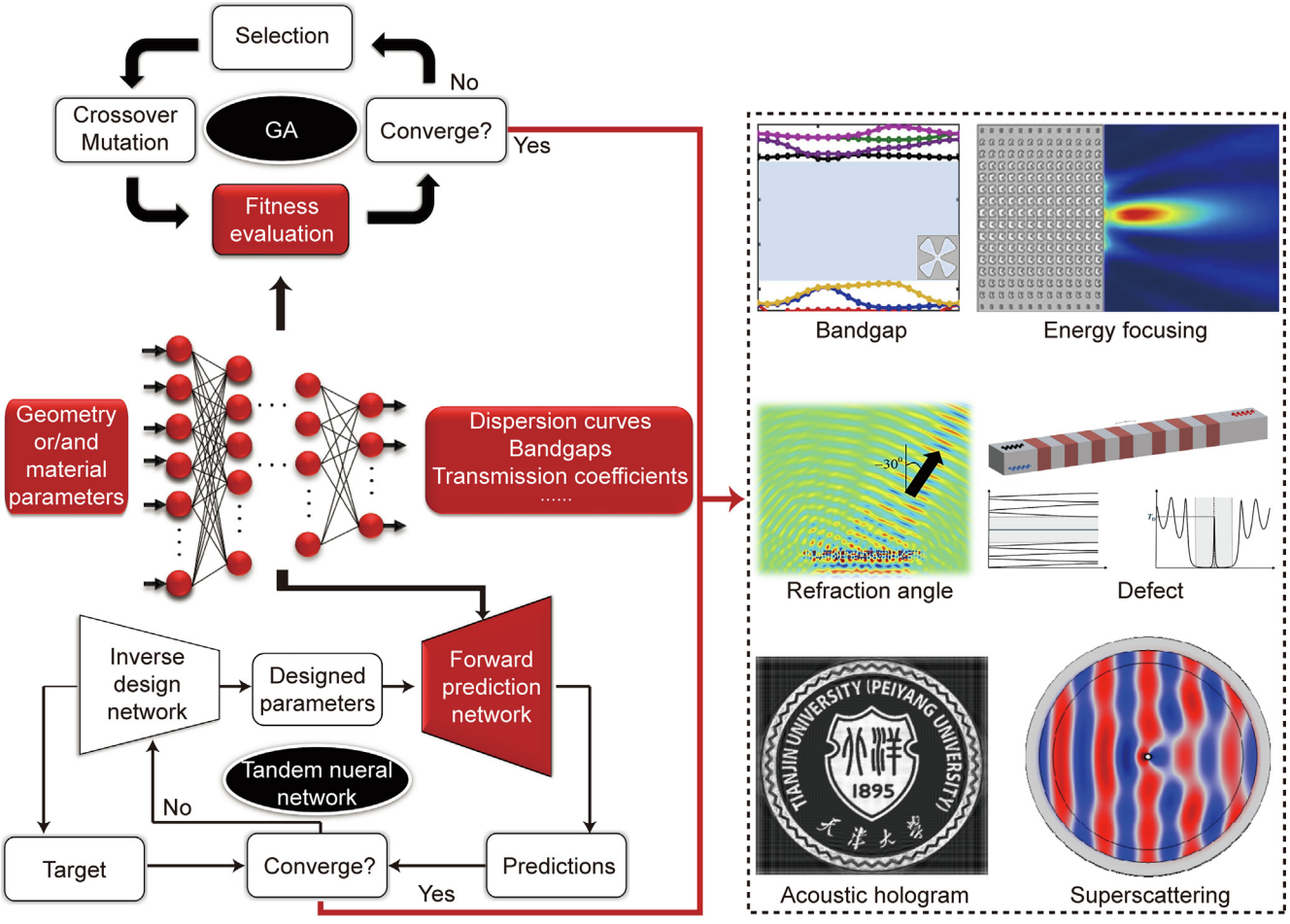

FIG. 7

Machine learning models based on forward prediction multilayer perceptron (MLP) for the parameter design of PMSMs, which mainly include the combination of GA and MLP and the tandem neural network. Reproduced with permission from Refs. [53,157–159,163,165].

Please cite this article in press as: H.-W. Dong et al., Materials Today, (2024), https://doi.org/10.1016/j.mattod.2024.09.012

Data-driven machine learning

In current machine learning models for PMSMs, data-driven approach is the mainstream since it only requires data rather than complex physical equations. The data are normally generated by numerical calculation methods [156], such as the finite element method and plane wave expansion method. Machine learning models can be trained with these data. They can efficiently single out expectational PMSMs from their generalization space according to the target. Depending on the properties of design variables, the design of PMSMs can be categorized into parameter design and topology design. The former is normally lower-dimensional and continuous, while the latter is high-dimensional and discrete.

For the parameter design of PMSMs, machine learning models based on forward prediction multilayer perceptron (MLP) are very effective, as shown in Fig. 7. The MLP is trained with geometrical or material parameters of PMSMs as input and target properties (e.g., dispersion curves/bandgaps and transmission coefficients) as output. The forward prediction MLP, as a surrogate model, replaces the role of numerical simulation methods, thus significantly reducing the calculation time for PMSMs to millisecond level. Therefore, the time taken for inverse design using suitable optimization algorithms and forward prediction MLP can be significantly shortened to just a few seconds. This approach has been used to successfully design wave refraction angles of multi-functional elastic metasurfaces [157], energy focusing of gradient-index phononic crystals [158], bandgaps of plate PnCs [159], megapixel acoustic hologram of metasurfaces [53], etc. Indeed, as a continuously differentiable function, the forward prediction MLP has the ability to design PMSMs [160]. In the MLP, the design parameters are independent variables, whilst the target properties are dependent variables. It should be noted that although the expected design parameters of PMSMs can be solved through the gradient-based backpropagation of the MLP, the model is reliable only within its limited generalization domain. Hence, it is necessary for MLP to constrain the range of design parameters by differentiable functions. A tandem neural network, comprising an inverse design network and a forward prediction network, namely a forward prediction MLP, can constrain design parameters through the activation function in the last layer of the inverse design network [161]. During its design process, a desired property was input into the inverse design network, generating design parameters within constrained ranges. These design parameters were then fed into the forward prediction MLP, outputting the corresponding property. Iteratively, the design parameters were adjusted using the backpropagation driven by the disparity between the desired and predicted properties, until the predicted property matches the desired one. Wave absorption [162], sound super-scattering [163], topological bandgaps [164], narrowband filtering [165], and wavefront modulation [153] of PMSMs have been designed by using tandem neural network. In addition, an MLP trained with targets as input and design parameters as output can realize the parameter design of PMSMs [166], but its training is difficult to converge for complex problems since the inverse design is normally a one-to-many non-mapping problem. Reinforcement learning was also used to design parameters of PMSMs [167]. Nevertheless, it is better at strategic decision-making and is more suitable for the real-time control of smart PMSMs.

For the topology design of PMSMs, machine learning models based on generative networks are necessary to handle the high dimensionality and discreteness of topologies, as shown in Fig. 8. Variational autoencoder (VAE) [168] and generative adversarial network (GAN) [169] are two classic generative models. A VAE consists of an encoder and a decoder. Relying on the compression effect and probability sampling of the bottleneck layer which connects the encoder with decoder, the VAE can transform the topology space of PMSMs into lower-dimensional and

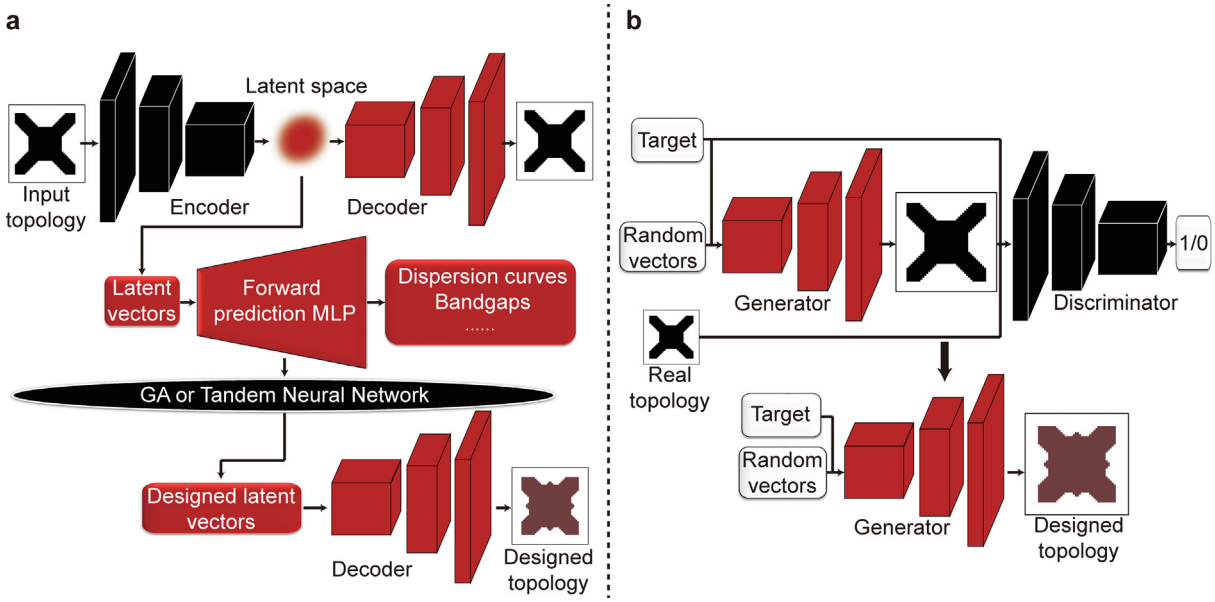

FIG. 8

Machine learning models based on generative networks for the topology design of PMSMs. (a) Variational autoencoder-based model; (b) Generative adversarial network-based model.

Please cite this article in press as: H.-W. Dong et al., Materials Today, (2024), https://doi.org/10.1016/j.mattod.2024.09.012

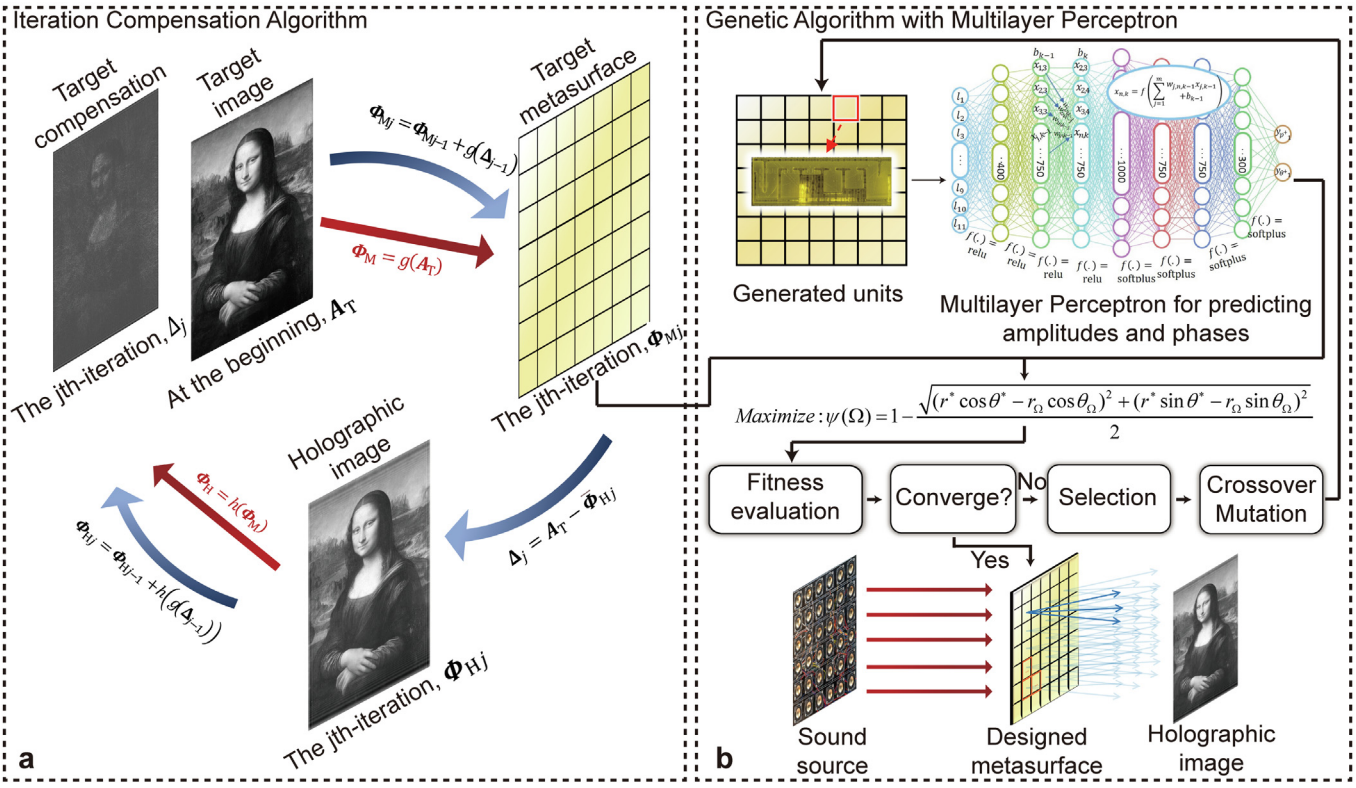

FIG. 9

Inverse design of acoustic megapixel-metasurfaces-enabled holography based on data-driven deep learning. (a) Iteration compensation algorithm for exploring the required distribution of phase and amplitude. (b) GA combined with deep learning model for designing a large-scale metasurface with four-million microstructures. Reproduced with permission from Ref. [53].

continuous latent space. Therefore, a latent vector can substitute a topology, which means designing latent vectors can realize the topology design of PMSMs. The design approach of latent vectors can refer to the parameters design of PMSMs because the data characteristics of latent vectors are the same as those of design parameters. For example, a VAE was used to compress 50×50 topologies of phononic crystals into 1×3 latent vectors using a simplified tandem neural network [170]. The decoder of the VAE was used to convert the designed latent vectors back to corresponding topologies. The design of latent vectors can also be realized by the combination of GA and forward prediction MLP [171]. A GAN, consisting of a generator and a discriminator, is trained through the competitive process of the two models. GAN can be used to generate high-quality topologies, but it is less adept at handling data with physics. Therefore, conditional GANs were employed to design topologies of PMSMs [172,173]. During the training of a conditional GAN, physical information, such as bandgaps and transmission coefficients, is taken as conditions to input into the generator and discriminator. The trained generator can design topologies of PMSMs according to input random vectors and conditions, namely targets. This training establishes the mapping from targets and random vectors to topologies, where the input of random vectors in conditional GANs addresses the nonconvergence problem caused by the one-to-many non-mapping inverse design. Furthermore, the forward prediction neural networks trained are effective in filtering PMSMs designed by conditional GANs [174,175], improving the design accuracy. While conditional GANs can realize quantitative designs, they may not excel at qualitative designs, such as maximizing bandgap width, since the form of the input target is fixed. On the other hand, the aforementioned VAE-based model can achieve quantitative and/or qualitative designs because the target form can be changed by modifying the objective function.

To realize a megapixel acoustic hologram using a metasurface with millions of microstructures, as shown in Fig. 9, an iterative compensation algorithm was proposed to remove the interference fringes and unclear details of the images for the near-perfect resolution [53]. After obtaining the required distributions of phase and amplitude, a deep neural network was constructed to inversely design the bi-anisotropic microstructures on demand. As a result, a megapixel image of Mona Lisa's portrait was reconstructed by a 2000×2000 metasurface-based hologram.

Physics-informed machine learning

Although data-driven machine learning models have shown remarkable success in the inverse design of PMSMs, they necessitate big labeled data, resulting in significant workload. Additionally, their design spaces are constrained by training data, inhibiting exploration of novel structures, and it is challenging to assess the credibility of designs since the error cannot be evaluated directly. Recently, physics-informed machine learning [176] has been widely used in the design of materials and structures [177–179]. It harnesses domain-specific knowledge on the

Please cite this article in press as: H.-W. Dong et al., Materials Today, (2024), https://doi.org/10.1016/j.mattod.2024.09.012

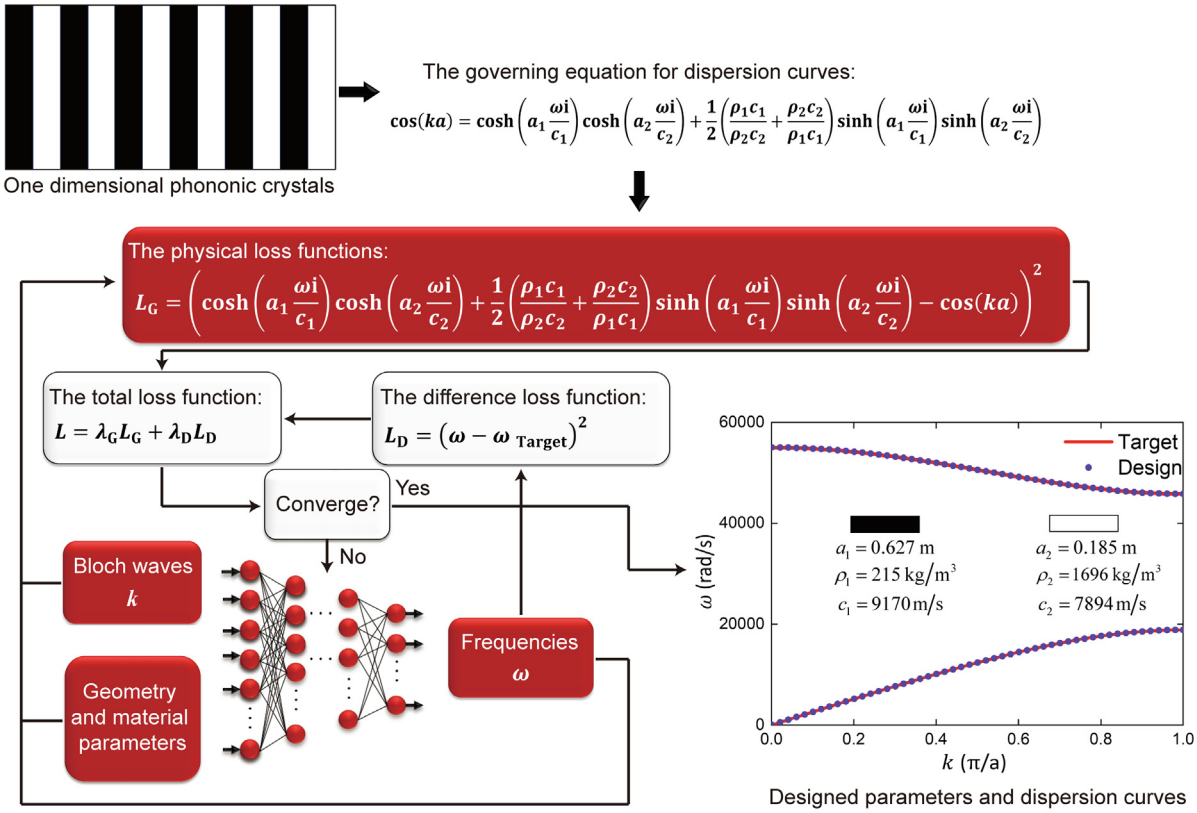

FIG. 10

One example for the physics-informed machine learning designing 1D PnCs, where vertically incident S waves are considered.

underlying physical laws or equations governing a system to guide and augment the learning process [176]. Since the embedded physical equations effectively govern the generalization domain, physics-driven machine learning has the potential to accurately learn law governing PMSMs even with limited or no available labeled data. Due to the broad generalization domain controlled by governing equations, physics-informed machine learning is more conducive to the exploration of novel PMSMs. Residual terms of the physical equations can assist physics-driven models in judging the credibility of designed PMSMs. Compared with traditional numerical methods, the physics-informed machine learning offers the advantages of machine learning and in the meantime incorporates more insights into the real physical problems by defining the constraints. In particular, the physics-informed neural network has remarkable advantages in inverse problems. To solve inverse problems, traditional numerical methods need to be combined with optimization algorithms, such as SIMP, GA and level set method, etc. In this way, lots of numerical simulation models need to be solved, and each model requires many iterations to make residuals of governing equations small enough. Therefore, there are a lot of numerical calculations if traditional numerical methods are used to handle inverse problems. However, as a differentiable function, the physics-informed neural network can solve inverse problems by taking the derivative of its internal parameters, which is similar to that of solving the independent variables of a function by gradient descent. Hence, for inverse problems, the physics-informed neural network only requires solving a single model rather than several models, leading to high efficiency and low computational effort. Physics-informed machine learning has been applied to the design of photonic or electromagnetic metamaterials [180–182]. Although elastic waves exhibit greater complexity in terms of degrees of freedom, vibration modes, dispersion, etc., compared to light or electromagnetic waves, they share certain similarities in the forms of the wave equations. Hence, physics-informed machine learning designing PMSMs is feasible in theory although there is currently no reported research in the field of PMSMs. For example, the governing equation for dispersion curves, derived from the transfer matrix method [183], can be incorporated into an MLP to create a physics-informed machine learning model for designing 1D PnCs, as shown in Fig. 10. The governing equation was transformed into a physical loss function. In this MLP, the input contains geometrical and material parameters as well as Bloch waves, and the output is frequency. These physical variables can be imported into the physical loss function, ensuring the compliance of the output frequencies with physical constraints. A difference loss function needs to be established to ensure the output frequencies closely match the target dispersion curves. As illustrated in Fig. 10, results from the physics-informed MLP are satisfactory, proving the feasibility of the physic-informed approach for PMSM design.

Finally, machine learning can be driven by both physics and data [184]. This approach is a powerful technology for addressing

Please cite this article in press as: H.-W. Dong et al., Materials Today, (2024), https://doi.org/10.1016/j.mattod.2024.09.012

problems with a small number of data and incomplete physical information. It has been used to improve prediction accuracy greatly in situations where the amount of data is extremely small or when physical equations are not available [185,186]. Hence, the fusion of physics and data-driven machine learning holds great promise for enabling few-shot learning or exploring the inherent nature of PMSMs.

Like the reported studies on static structure optimization [187] and photonic metamaterials [188], ToP can be combined with machine learning to inversely design the PMSMs [189]. It is expected that some intractable challenges, such as mass training samples and excessive grid scale, need to be addressed when using ToP and machine learning simultaneously. In the future, the inverse-design methodology using multiple approaches could be an important development direction.

Other semi-empirical optimization techniques

In addition to topological inverse design through ToP or machine learning, existing studies also reported the inverse design of PMSMs through the optimization of pivotal featured parameters. Despite its inability to describe the whole topology of a PMM, this kind of inverse-design method can explore simple PMSMs with high-efficiency wave functionality with simple topology. The underlying basis of this method is the choice of suitable or proper topological feature parameters based on an in-depth understanding of the physical essence. For example, a bi-anisotropic acoustic scattering-free metasurface can be inversely designed by optimizing nine geometric parameters of multi-cavity metasurface elements based on a GA [65]. Similarly, the cylindrical bi-anisotropic metasurfaces with optimized several feature parameters can transform a monopole source into a spinning field with highly efficient angular momentum [190]. When the geometric parameters of a non-local metasurface are optimized, broadband impedance matching can be realized for the low-frequency ultra-broadband absorption [52]. Besides, broadband solid pentamode cloak can be designed by parameter optimization combined with the transformation theory [104]. When both the phase and amplitude shift are introduced,

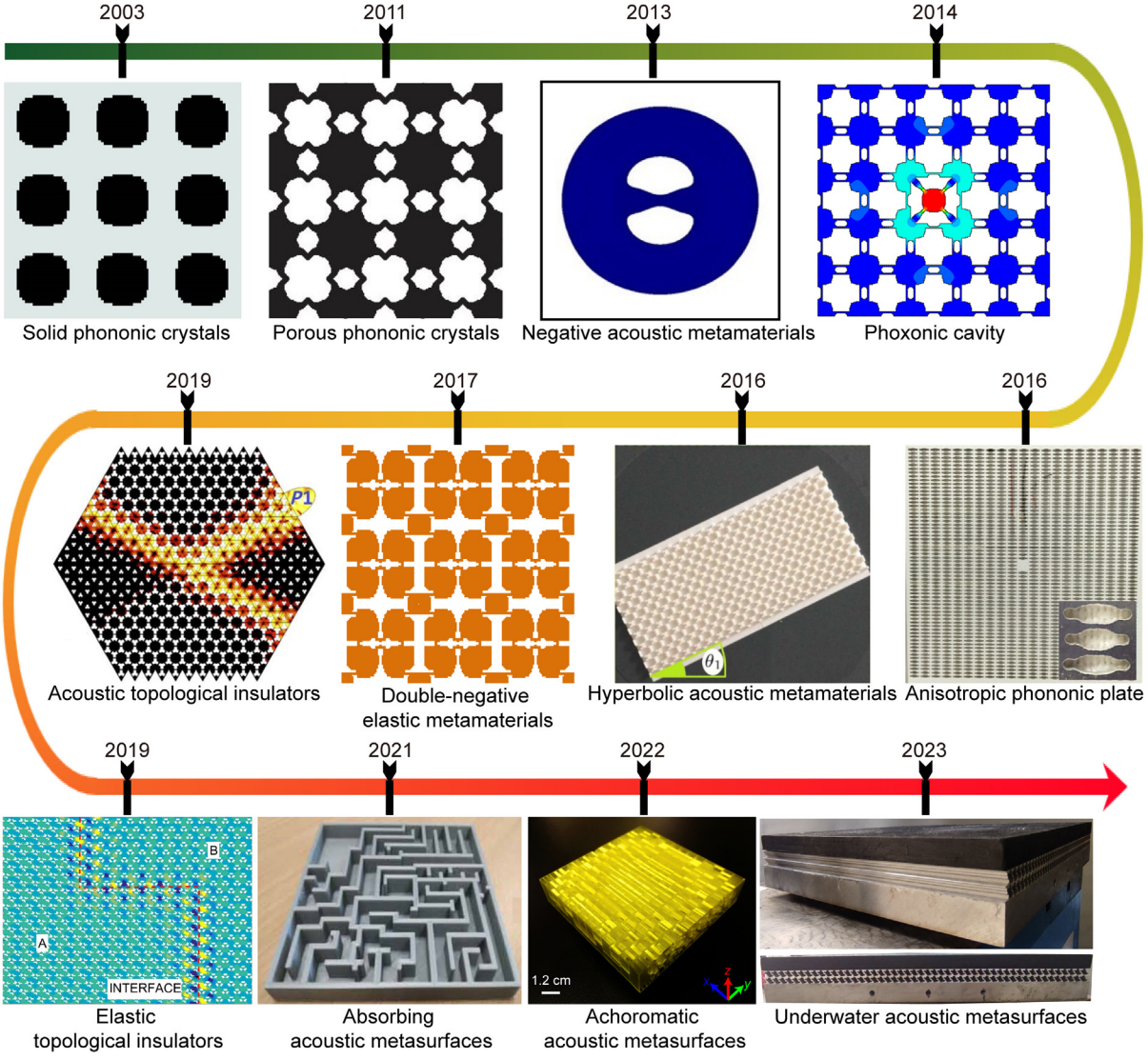

FIG. 11

Diversiform inverse-designed PMSMs from local to global responses. Reproduced with permission from Refs. [51,52,54,55,58,67,77,85,123,196,200,202].

Please cite this article in press as: H.-W. Dong et al., Materials Today, (2024), https://doi.org/10.1016/j.mattod.2024.09.012

high-efficiency elastic metasurfaces defeating the generalized Snell's law can be inversely designed by optimizing the geometric parameters of supercells [191]. In some cases, elaborate optimization of some geometric parameters of microstructures can also give rise to customized wave functionalities of new PMSMs. For complex inverse problems, however, it is insufficient to only rely on parameter optimization; therefore, one should resort to the powerful topological inverse design with expanded search space.

Inverse-designed PMSMs and customized functionalities

Inspired by the inverse design of electromagnetic and optical meta-structured materials [112,192–195], as illustrated in Fig. 11, the inverse design of PMSMs first started with the ToP of phononic crystals for bandgap engineering [51]. New wave devices were enabled when defects were introduced in phononic

TABLE 1

Summary of representative inverse-designed PMSMs.

Type of waves	Design domain	Fundamental quantities	Inverse-design method	Functionalities/applications	Key performances	Refs.
Bulk elastic	2D unitcell	Eigenfrequency	SIMP	Bandgaps, wave-stopping, waveguiding	22.5 % (Relative bandgap size)	[51]
Bulk elastic	2D unitcell	Eigenfrequency	GA	Bandgaps	62.6 % (Normalized bandgap size)	[196]
Airborne acoustic	2D unitcell	Refractive index, impedance	GA	Focusing	1–2.45 (Refraction index range)	[205]
Bulk elastic	2D unitcell	Eigenfrequency	GA	Amplitude-dependent bandgaps	3.2 rad/s (Complete bandgap size)	[206]
Airborne acoustic	2D circular region	Scattering cross section	GA and simulated annealing	3D acoustic cloaking	90 % (Suppressing scattering waves)	[56]
Electromagnetic and bulk elastic	2D unitcell	Eigenfrequency	NSGA-II	Phoxonic bandgaps, phoxonic cavity	72.3 % (Phononic) and 14.1 % (Photonic)	[67]
Bulk elastic	2D unitcell	Eigenfrequency	NSGA-II	Lightweight and large complete bandgaps	106.8 % (Complete bandgap size)	[207]
Bulk elastic	2D unitcell	Isofrequency curve	SIMP	Non-diffractive self-collimation	Collimation along 30°	[75]
Flexural	2D unitcell	Group velocity	SIMP	Directional transmission	Group velocity ratio exceeding 1.8 in [27.5 kHz, 32.5 kHz]	[77]
Waterborne acoustic	2D plane	Phase and amplitude	Iterative angular spectrum	Underwater acoustic hologram	15000-pixel (Asymmetric particle assembly)	[16]
Airborne acoustic	2D region comprising periodic unitcells	Refractive beam energy	SIMP	Acoustic negative refraction for varying frequency and angle of incidence	≈98 % (Negative-refraction transmittance)	[80]
Bulk elastic	2D microstructure	Effective density and elastic modulus	GA	Broadband negative refraction and anisotropy	7.91 kHz (Double-negative range size)	[54]
Bulk elastic	3D unitcell	Eigenfrequency	GPU-accelerated SIMP	Bandgaps	100.03 % (Normalized bandgap size)	[135]
Airborne acoustic	2D region comprising periodic unitcells	Wave intensity	SIMP	Backscattering-protected pseudospin acoustic energy transport, splitter	≈12.5 % (Relative topological bandwidth)	[123]
Bulk elastic / Waterborne acoustic	2D microstructure	Effective density, elastic modulus, impedance	GA	Water-like low-scattering, underwater sound isolation	>150 % (Relative range size of single mode)	[138]
Airborne acoustic	2D cavity including lattice sites	Absorption coefficient	Convolutional neural network	Acoustic absorber	100 % absorption with ultrathin thickness (λ/684)	[202]
Airborne acoustic	2D microstructure	Transmissive phase and amplitude	GA	Acoustic deflection/ focusing/ levitation	120 % (Relative bandwidth of achromatic functionality)	[52]
Airborne acoustic	Five parameters of two resonators	Sound absorptance	GA	Sound insulation	99.1 % (Radiated sound absorptance)	[208]
Bulk elastic/ Waterborne acoustic	2D microstructure	Effective density, elastic modulus	GA	Underwater sound absorption, insulation	>80 % (absorption) and 20 dB (insulation) (Broadband range of 2–10 kHz)	[85]
Airborne acoustic	Eleven parameters of an anisotropic element	Transmissive phase and amplitude	Deep neural network	Acoustic hologram	4-million pixel (Resolution of a hologram image)	[53]

Please cite this article in press as: H.-W. Dong et al., Materials Today, (2024), https://doi.org/10.1016/j.mattod.2024.09.012

crystals or when the coupling among different waves was considered. As a result, some representative functions such as wide bandgaps [196], high-efficiency optomechanical coupling [67] and directional energy propagation [77] were realized. Subsequently, with the development of meta-structed materials possessing exotic dynamic effective parameters (negative mass

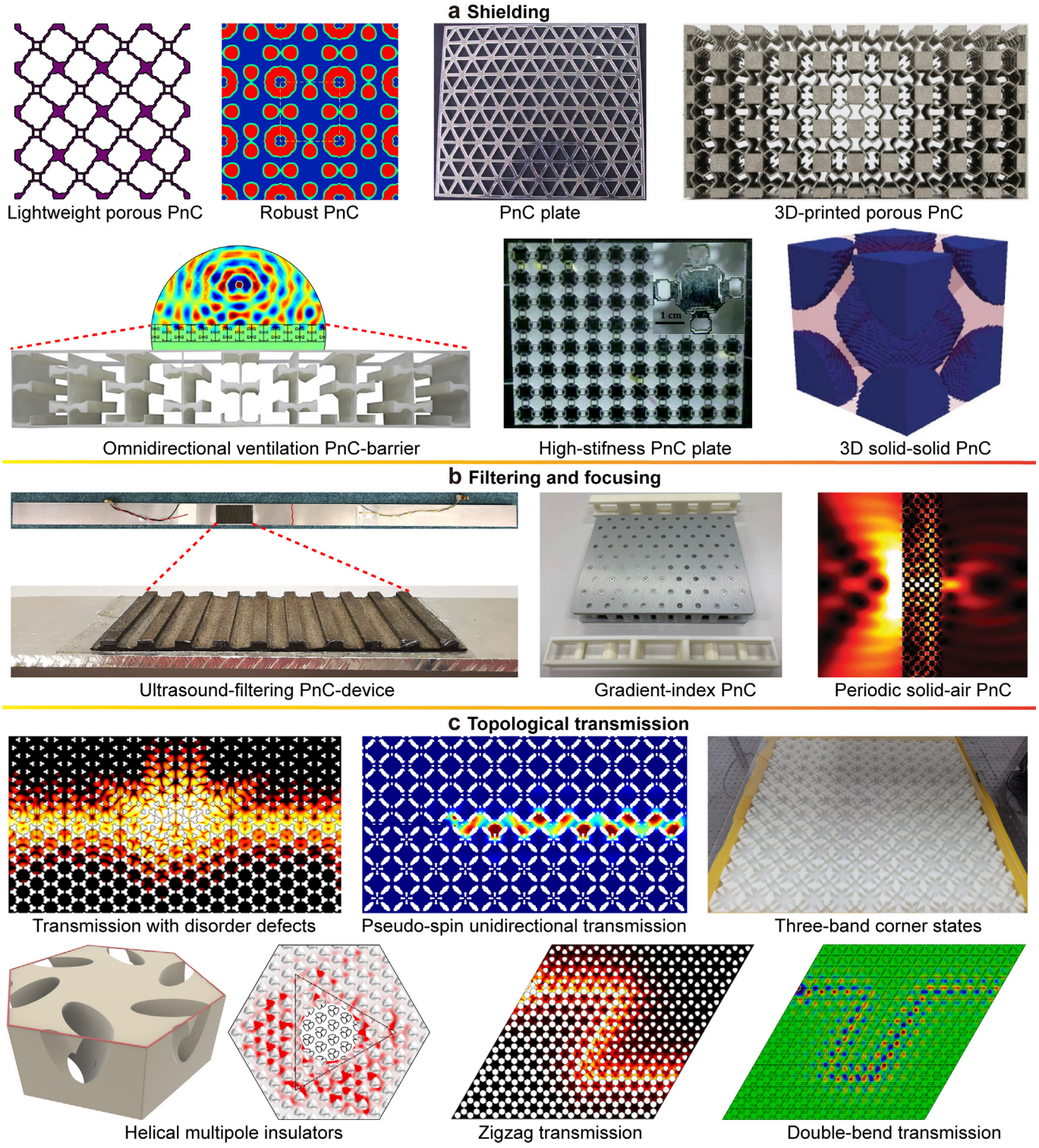

FIG. 12

Inverse-designed phononic crystals (PnCs) and topological insulators. (a) Various 2D and 3D PnCs for elastic/acoustic wave shielding. Reproduced with permission from Refs. [134,216,217,227]. (b) Surface-mounted PnC-device for elastic filtering, gradient/periodic PnCs for imaging and focusing. Reproduced with permission from Refs. [76,242,243]. (c) Elastic/acoustic topological insulators for different kinds of topological transmissions. Reproduced with permission from Refs. [78,79,123,247,251,252].

Please cite this article in press as: H.-W. Dong et al., Materials Today, (2024), https://doi.org/10.1016/j.mattod.2024.09.012

density [11,59,197], negative modulus [94], double-negativity [96], zero mass density [198] and strong anisotropy [89,199], etc.), research effort has been shifted to the ToP of elastic [54] and acoustic [200] metamaterials exhibiting exotic functionalities such as broadband negative refraction [54,124] and subsequent subwavelength imaging [54] facilitated by the realization of the negative refraction. Research interest has also been extended to the ToP of acoustic [52] and elastic [201] metasurfaces for the control of the phase, amplitude, and polarization with reduced footprint. Additionally, machine learning was utilized for constructing millions of microstructures [53]. These approaches brought about some representative functions including ultra-broadband abnormal deflection [52], focusing [52], absorption [202], hologram [53], ultrasound levitation [52], and underwater sound stealth [85]. Recently, the surge of acoustic and elastic topological insulators with unconventional edge states offered new opportunities for controlling waves efficiently. Representative works have showcased broadband quantum spin Hall effect [55,58] and chirality-based unidirectional transmission [66,78] through inverse design using ToP [55,203] or machine learning [204]. Within a time-span of 20 years, the inverse design of PMSMs gradually expanded from conceptual design to the materialization of numerous customized wave functionalities. The scope also shifted from periodic microstructures to aperiodic/gradient/hierarchical microstructures and macrostructures, encompassing intrinsic physical parameters to local–global responses. Overall, this research field has entered a booming period that could be the vital prelude to the practical applications of PMSMs on demand. Details about some representative inverse-designed PMSMs are summarized in Table 1.

Note that the contents in Sections of "Phononic crystals and phononic topological insulators", "Phononic metamaterials", and "Phononic metasurfaces" show diverse PMSM-enabled functionalities, which are different from the so-called applications shown in Section of "Applications of customized PMSMs". In fact, the discussions about functionalities in the first three sections emphasize the laboratory-level proof of concept and verifications of the fundamental functionalities. However, the last section highlights the representative engineering technologies based on the excellent functionalities of PMSMs, not just the phononic functionalities themselves. In other words, the representative works mainly validate the effectiveness of technologies, rather than functionalities. The works discussed in Section of "Applications of customized PMSMs" are closer to the practical application requirements.

Phononic crystals and phononic topological insulators

Periodic arrangements of scatterers can lead to the suppression of transmitted waves at certain frequencies based on the band structures [61]. This property was initially studied by Sigmund and Jensen in 2003 in the context of topology-optimization methodology, where 2D solid–solid phononic crystals based on the solid isotropic material with penalization were proposed [51]. Their studies discovered new phononic crystal topologies and realized broadband elastic wave bandgaps, showing the enormous potential of ToP in the design of composite materials and structures. Subsequently, abundant studies reported the ToP of various phononic crystals for bandgap engineering, as shown in Fig. 12.

Bandgap engineering

- **Bandgap forms.** In terms of bandgap forms, some studies reported in the literature aimed at maximizing the bandgap between two adjacent bands [196,209,210]. Other studies considered the simultaneous optimization of multiple bandgaps for achieving wave filtering within multiple frequency domains [211]. When optimizing the bandgaps for out-of-plane mode, optimized phononic crystals exhibit interesting geometrical principles, i.e., the total number of the scatterers equals the integer times of the serial number of the bandgaps; and the centers of all scatterers form a typical Voronoi diagram [209]. Generally, the real and imaginary parts of wave vectors characterize the dispersion relations and attenuation characteristics of wave propagation, respectively. If the imaginary part of wave vectors is targeted, the ToP of unit cells with the prescribed quantitative imaginary wave vectors along different directions can create unidirectional acoustic transmission [69]. Combined with a guide-rail reconstruction system, optimization of several phononic bandgaps can create multi-state tunable phononic crystals [212]. In addition, it was found that certain randomness of the phononic crystals could support one or multiple bandgaps at a prescribed location of the arbitrary band structures by inversely designing phononic networks [213]. Recently, the inverse design of band structures using nonlocal interactions demonstrated that single-band and double-band dispersion curves can be accurately achieved, even for the multiple roton/maxon and undulation critical points, showing the robust tailoring capability of dispersion relations [74].
- **Single-/multi-phase constituent materials.** From the perspective of constituent materials, existing ToP studies entail solid–solid [51,209,214,215], solid-air (Fig. 12a) [196,207,216,217], and three-phase solid [218] phononic crystals for single and multiple low-frequency broadband bandgaps. In addition to the metallic materials and high polymer materials, smart materials such as piezoelectric materials were introduced in the optimization problem to control the optimized bandgaps [215]. Since the fluid–solid coupling is very sensitive to the topologies of edges, very few studies reported the ToP of fluid–solid phononic crystals. It is worth mentioning that optimized porous phononic crystals can support ultra-broadband low-frequency bandgaps with ultralight weight [134], see Fig. 12(a). By virtue of the multi-objective optimization algorithms, it is effective to create multifunctional porous phononic crystals blending the light weight, high stiffness, and body-wave/lamb-wave bandgaps [219]. The optimized three-phase phononic crystals can further decrease the bandgap frequency regions for the low-frequency wave manipulation [220]. When nonlinear stress–strain property was considered, the optimization could generate nonlinear porous phononic crystals with broadband bandgaps [206]. Using hyperelastic materials, the ToP of unitcells can create tunable bandgaps between two preselected modes in the deformed configuration [57].
- **Diverse inverse-design methods.** In terms of inverse-design approaches, representative gradient algorithms, such as SIMP [51,75,121,216], level set [221], and BESO [222–

Please cite this article in press as: H.-W. Dong et al., Materials Today, (2024), https://doi.org/10.1016/j.mattod.2024.09.012

224], etc., were usually employed to design phononic crystals with relatively low computational cost. Non-gradient heuristic algorithms, such as GA [209], particle swarm, and simulated annealing, can realize the required bandgaps on demand as well, especially for strongly nonlinear or discontinuous non-convex problems. To improve the optimization efficiency and reduce the difficulty of optimization, some studies utilized the approximation model such as the fuzzy theory and surrogate models [210,225]. These models, however, are challenged to tackle uncertainties in the construction of unit-cells, which will evidently affect the resulting band structures of the inversely designed phononic crystals. Obviously, an imperfect interface impacts on the resulting band structures [226]. In this case, the ToP based on phase field can be utilized to generate phononic crystals with typical diffuse region uncertainties, thus obtaining robust bandgap characteristics [227] (Fig. 12(a)). Likewise, a level set-based interface-enriched approach can also build phononic crystals with smooth and non-diffuse boundaries [221]. During the last few years, data-driven and physics-informed machine learning has provided an intelligent paradigm for customizing band structures of phononic crystals [167,175,228–231]. Combining a high-precision and robust deep neural network model with GA can accurately generate the desired bandgap bounds for two-phase phononic crystals [228].

- **Design domain.** As for the design domain, most studies focused on 2D ToP with certain symmetric conditions. The assumption of asymmetric symmetry facilitates the generation of wider optimized bandgaps despite the greater computational cost [210] (Fig. 12a). Very few studies attempted the ToP of 3D limited-pixel phononic crystals (Fig. 12a) [135,221,223]. This could be explained by the fact that 3D optimization significantly increases the evaluation cost within an expanded design space, thus leading to slower convergence, harder topological description of structures, and more stringent manufacturing requirements.
- **Typical waveforms.** From the perspective of waveforms, most researchers reported the elastic bandgaps of longitudinal waves, transverse waves, flexural waves, Lamb waves, and surface waves. If multiple wave modes are required to be prohibited, complete full-mode bandgaps can be optimized to significant wave insulation [207]. Similarly, it is also useful to employ the similar inverse design to obtain bandgaps for the filtering of specific part of the wave modes. When the ToP of phononic-crystal plates was conducted, the large bandgaps for the fundamental asymmetric, symmetric, or mixed guided wave modes can be systematically generated for the attenuation or transmission of different wave modes [219] (Fig. 12a). Fewer studies investigated the optimization of coupled electromagnetic and acoustic waves, such as the simultaneous phononic and photonic bandgap engineering [67]. The optimized phoxonic bandgaps can be used to construct high-efficiency optomechanical cavities for new biological transducers, force/mass/acceleration sensing and optically microwave oscillators [3,232–235]. While optimized bandgaps of elastic waves are promising for low-frequency vibration isolation, ultrasound non-destructive testing with filtering properties, anti-seismic damage, and so on, an area that warrants further investigation is the bandgap optimization under the fluid–solid coupling [236].
- **Commonly adopted optimization quantities.** In general, dispersion relation is the most commonly used optimization quantity. The transmission spectrum as a typical full-wave response was also usually utilized to design phononic crystals by evaluating how much attenuation is induced. For example, minimizing the average displacement amplitude on the boundary led to an up to support 70 dB attenuation of wave signals [51]. The approach was later extended to the propagation of shock waves by designing phononic crystals that can minimize the transmissibility of an incident general transient pulse [71,237]. Combining a tailored transmission spectrum with bandgaps can bring about topology-optimized airborne phononic crystals acting as a broadband near-omnidirectional acoustic ventilation barrier [238] (Fig. 12(a)). In the past few years, several studies reported the synthesis of neural network models and transmission spectrums through inversely designed phononic crystals. For instance, invertible neural networks can be adopted to predict and design the transmission spectra of the 1D drill-pipe phononic crystals [239]. Similarly, maximizing the transmission at a target frequency can generate high-efficiency narrowband filters [165]. When nonlinear effect is considered, both the convolutional neural network and generalized regressive network can realize the efficient inverse design of nonlinear phononic crystals for customized second-order wave transmission spectra [240]. Notably, concurrent multi-scale optimization, in which ToP of different phononic microstructures and macroscopic topology are simultaneously involved, is also proposed to prevent waves from propagating within the prescribed frequency ranges [121].
- **Other quantities.** Other wave characterization quantities such as refractive index, group velocity, and equal-frequency contour can be used for the inverse design of phononic crystals. A Reissner-Mindlin plate model with optimized effective index distribution can contribute to an energy harvesting system [241]. Since the group velocity characterizes the energy propagation, a topology-optimized perforated phononic-crystal plate with strong anisotropy can be realized through ToP by controlling the group velocities along two principal directions [77]. In addition, ToP based on equal-frequency contours can give rise to customized wave functionality. For instance, the zero diffraction of incident waves and self-collimation phenomenon along a customized direction can be achieved through the ToP of phononic unit cells with prescribed curvatures and slopes of equal-frequency contours [75].

During the past two decades, extensive efforts were made on the inverse design of bandgap engineering. However, some intractable questions remain open. For example, how to realize the large-scale 3D inverse design? How to reduce the structural complexity during inverse design as low as possible? Is it possible to conduct the inverse design of soft phononic crystals for required buckling modes and bandgaps? How to realize the

Please cite this article in press as: H.-W. Dong et al., Materials Today, (2024), https://doi.org/10.1016/j.mattod.2024.09.012

inverse design of nanoscale phononic-crystal devices considering the size effect? Meanwhile, it is a generic yet challenging problem to perform inverse design in multiple physical fields. Interestingly, it is possible to utilize data-driven and physics-driven machine learning for customizing the multiple arbitrary dispersion curves and even all wave-vector modes.

Filtering and focusing

To achieve wave filtering using phononic crystals, a usual practice is to introduce the transmission spectrum or energy flux into optimization model. If the band structures are combined with particular equal-frequency contour, broadband focusing can be achieved as well. Considering suitable defect modes and transmission spectrum, high-Q and high-efficiency elastic filters based on phononic crystals can be inversely designed by minimizing the elastic wave flux at the output port of a waveguide [73]. Similar concepts are found in engineering transmission spectra of surface waves, where a high-efficiency surface wave filter at 0.61 MHz was realized by minimizing the transmission based on total displacements in the terminal region [46]. The optimized aperiodic device not only supports the Bragg-grating effect but also induces mode conversion from surface waves to longitudinal or transverse waves [46]. Other design concepts were also incorporated into the phonic crystal structure design, including the introduction of a specific gradient and coating components (Fig. 12b) [242], giving rise to wave-focusing capabilities. When a customized phononic crystal with multiple bandgaps was designed, the ultrasound Lamb-wave filtering and single-mode transmission could be reached through a simple surface-mounted phononic-crystal device (Fig. 12b) [243]. Maximizing the radius of the equal-frequency contour via a bi-directional evolutionary structural optimization method, on the other hand, achieves broadband all-angle negative refraction for focusing (Fig. 12b) [76].

The above studies on filtering generally lacks experimental verifications, let alone the inverse design and realization of high-Q acoustic surface wave devices. As for focusing, only 3D focusing were achieved by inverse-designed phononic crystals. It is necessary to combine phononic crystals and medical ultrasonic techniques. Depending on the propagation media (soft material, porous solid filled with liquid), inverse design of phononic crystals supporting high-efficiency shear waves to realize broadband high-resolution ultrasound imaging technologies, e.g., intracranial ultrasound, cardiac ultrasonic contrast, and arterial contrast ultrasound, etc., is also much needed.

Topological wave propagation

All the above wave properties and functionality are based on the bandgaps, defect modes and group velocities stemming from the band structures. On the other hand, when robust edge states are formed by breaking the symmetry of the lattices, phononic topological insulators can be realized which unfolded the astonishing feature of topological wave transmission immune to backscattering [8], one-way perfect transmission [244] and cross-waveguide splitter [8], etc.

In general, the introduction of symmetry breaking at the Dirac point can induce the quantum-like spin Hall effect. Alternatively, the introduction of non-zero Berry curvature can produce chiral valley pseudo-spin states. Nevertheless, since the design of topological states requires elaborate eigenstate and dispersion manipulation, empirical design has restricted the provision of novel topological insulators and functionalities. In 2019, the level-set-based ToP was applied to design phononic topological insulators. Through the optimization of eigenfrequency, the mechanisms of band zone folding and symmetry breaking were shown to create elastic topological insulators for flexural waves, showing the unique advantages of inverse design in constructing customized topological interface states and topological devices [58]. Using similar inverse-design strategy, the introduction of piezoelectric materials can contribute to reconfigurable piezoelectric topological phononic plates [245]. The inverse design based on the optimization of eigenfrequency also give rise to zigzag-interfaced valley Hall insulators [246] and multiband second-order sonic topological insulators with three-band corner states (Fig. 11c) [247]. Through combining machine learning with bandgap optimization, topological metaplates for flexural waves [248] and topological phononic beams [164,246,249] can be inversely designed as well. Unlike eigenstate-enabled inverse design, optimizing field intensity magnitude directly based on the acoustic intensities at different ports can contribute to the acoustic topological insulator with pseudospin-1/2 states, high transmission with a bandwidth of 12.5 %, even when disordered defects were introduced (Fig. 12c) [55]. This top-down inverse design dispensed with the constraints regarding topological acoustics, showing the universality of constructing on-demand topological-insulator devices. Using the intrinsic physical quantities of Berry curvature, chiral phase vortex, degenerate-state quantitative index, bulk polarizability and symmetry index, a series of quantum valley hall topological insulators [66], spin-hall topological insulators [250], 2D high-order topological insulator [251] and 3D spiral high-order topological insulators (Fig. 12c) [251] have been inversely designed. Alternatively, the inverse design based on the local density of states also successfully created multiple topological insulators. For example, the typical multiple-stage inverse design that involves maximization of the local density of states and non-trivial unitcell optimization has been fruitful in generating square-latticed acoustic pseudo-spin topological insulators (Fig. 12c) [78] and triangle-latticed pseudo-spin topological insulators [79,252] that support corner states (Fig. 12c) [247], pseudo-spin unidirectional propagation (Fig. 12c) [78], zigzag robust transmission [79] (Fig. 12c) and double-bend transmission (Fig. 12c) [252], etc. In addition, if the equivalent Hamiltonian was optimized, the square-latticed Dirac cones and quantum spin-Hall topological insulators could be realized as well [253].

Despite the diverse features and functionalities arising from the inverse-designed phononic topological insulators, many issues are still not settled or considered. For the inverse design of Dirac cones, reported studies can create four degenerate states at most. It may be possible to break through the current design to reach six or eight degenerate states, which will provide more plentiful topological physics. In addition, the existing inverse design of topological insulators only aimed at the linear and Hermitian systems. Future inverse design can consider the non-Hermitian topological effect, non-linear, non-Abelian, and topological defects [254], etc. In the future, inverse design of phono-

Please cite this article in press as: H.-W. Dong et al., Materials Today, (2024), https://doi.org/10.1016/j.mattod.2024.09.012

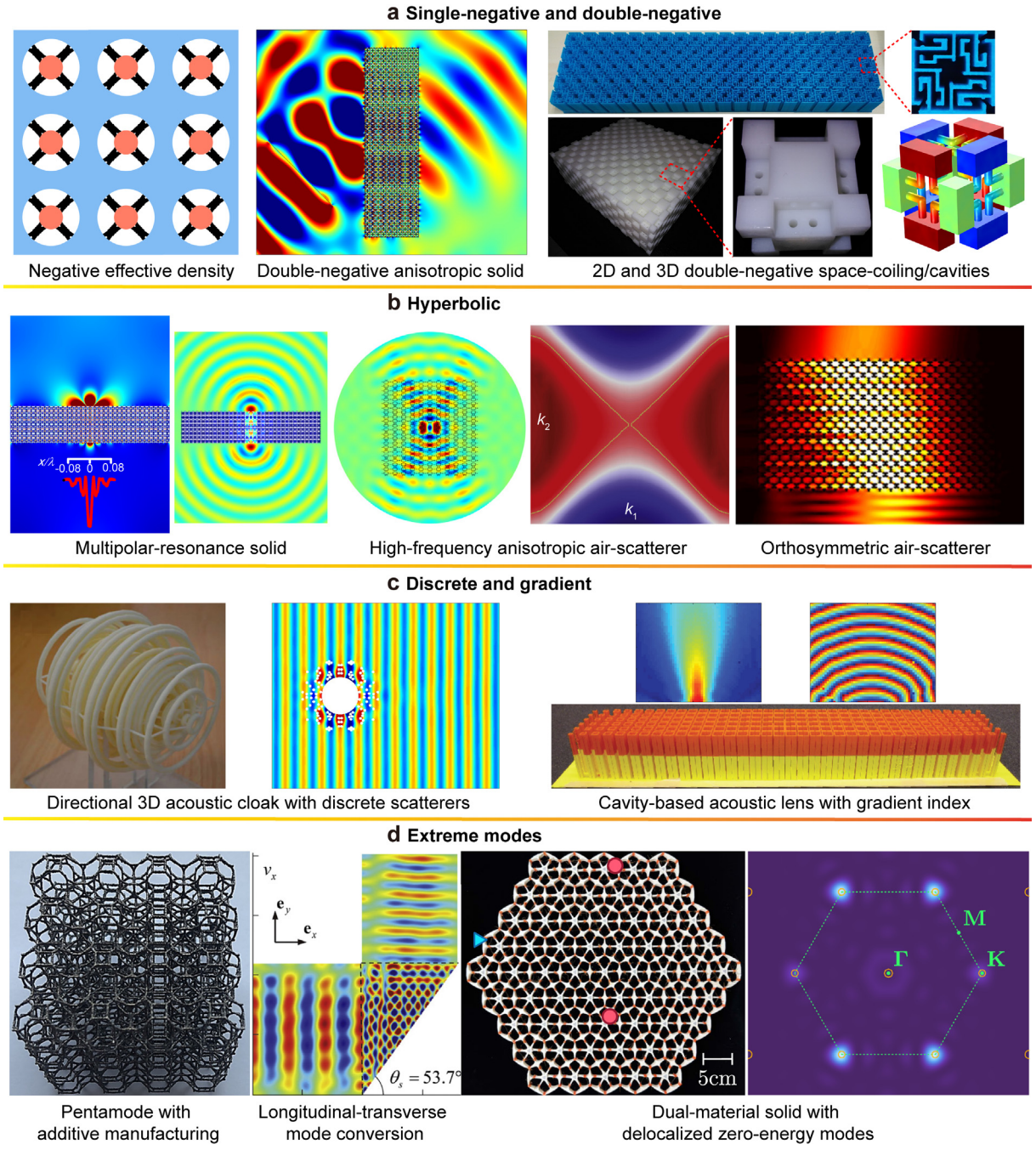

FIG. 13

Inverse-designed phononic metamaterials. (a) Metamaterials with single negativity and double negativity for 2D/3D system. Reproduced with permission from Refs. [54,98,99,255]. (b) Hyperbolic elastic metamaterials and acoustic metamaterials for super-high-resolution imaging, directional transmission, or negative refraction. Reproduced with permission from Refs. [80,258,260]. (c) Acoustic metamaterials with discrete scatters or gradient cavities for cloaking or superlensing. Reproduced with permission from Refs. [56,205]. (d) Elastic metamaterials with pentamode feature, longitudinal–transverse mode conversion, or delocalized zero-energy modes. Reproduced with permission from Refs. [68,267,272].

nic topological-insulator chips will be very exciting and full of applications.

Phononic metamaterials

As another category of periodic structures, metamaterials constitute subwavelength resonators or inclusions. The dynamic effective properties of these resonators or inclusions play a fundamental role in determining the collective behavior of the metamaterials in a homogenized medium perspective. The most intriguing properties of metamaterials, absent in nature, are exemplified by negative effective density, modulus, and refraction index. These unusual properties were first demonstrated based on resonating structures such as rubber-coated spheres, Helmholtz resonators, or plate structures [11,94,96]. From a macroscopic view, metamaterials can be directly modeled with an effective medium description. Because of these, many

Please cite this article in press as: H.-W. Dong et al., Materials Today, (2024), https://doi.org/10.1016/j.mattod.2024.09.012

unprecedented functionalities are directly associated with the exotic effective parameters realized by metamaterials. Examples include superlensing, subwavelength imaging, perfect tunneling and so on [35]. For a long time, how to construct suitable effective parameters has always been the central issue in the field of phononic metamaterials.

Negative effective properties

Since 2012 [205], the inverse design of phononic metamaterials with novel microstructures that interact with the wave has been successfully realized by using ToP and machine learning based on the dynamic effective parameters and wave propagation features of elastic/acoustic waves, e.g., the negative density (Fig. 13a) [255], near-zero density [54], negative bulk modulus [98,99,200,256], negative longitudinal or transverse modulus (Fig. 13a) [54], and strong anisotropy [92,99,124], etc. Owing to negative mass density, phononic microstructures show low-frequency resonant bandgaps that can be exploited for noise and vibration control (Fig. 13a) [255]. In this regard, efforts have been devoted to achieving anisotropic effective densities [93,257]. Based on the negative modulus, level-set method incorporated with minimizing imaginary and real components successively can bring about broadband negative effective bulk modulus for sound absorption [200]. This strategy can further optimize the negative effective bulk modulus with the definite acoustical-structure interaction [256]. Combining negative effective density and modulus produces even more versatile and unprecedented features, including broadband double-negativity (Fig. 13a) [54,99], hyperbolic features (Fig. 13b) [258], thus obtaining the broadband, high-efficiency negative refraction, directional transmission, and subwavelength focusing, etc. This idea has been tested for both acoustic and elastic waves [54,98,258], giving rise to high-resolution imaging and so on [99,258]. According to the presupposed refractive-index profile, the evolutionary optimization can bring about a maximized index of refraction, minimal frequency dependence of the material properties, and reduced acoustic impedance mismatch (Fig. 13c) [205]. When the ordering of microstructures was designed [259], it is possible to build machine-learning models that can quickly predict the phase velocities of elastic waves can design the digital ordering.

Unlike the above studies adopting the long-wavelength assumption, for the high-frequency cases, the high-frequency asymptotic theory combined with the level set method allows for the optimization of high-frequency homogenization tensor T_{ij} for accomplishing the customized hyperbolic features by exploiting resonances induced in the microstructures (Fig. 13b) [260].

Up to now, the inverse design of negative effective properties faces many challenging issues. The first obvious one is the need for a universal high-order dynamic effective homogenization scheme covering the low-frequency and high-frequency ranges. The homogenization needs to consider the local rotation modes, arbitrary wave vectors, and random asymmetry geometry. As such, the search space of the inverse design will be greatly increased, which potentially can be exploited for the discovery of band-new abnormal wave properties. If smart materials and active control are further deployed, realization of 4D phononic metamaterials by 3D inverse design would be a possibility. More importantly, the cluster-based machine learning can contribute to build the pool of phononic metamaterials with the systematic classification, and even guide the on-line inverse design of large-scale hierarchical metamaterials.

Low-loss cloaking

Optimizing "artificial structures" from the perspective of elastic or acoustic wave propagation characteristics, including scattering cross-section intensity, transmission spectrum, and far-field scattering [81], etc., can directly give rise to high-efficiency customized wave functionalities and features, naturally avoiding the conundrum regarding the dynamic homogenization of complex microstructures, especially chiral, asymmetric topologies, and local-rotation solids. One representative application is cloaking. For instance, for a system of multiple scatterers discretely distributed in the air, the optimization of the scattering cross-section intensity can entail directional 2D and 3D acoustic cloaks (Fig. 13c) [56,261]. In another example, using deterministic and probabilistic machine learning, optimizing the scattering cross-section spectra can generate a broadband acoustic cloak [152].

Current inverse design of acoustic cloaks is based on gradient design, which limits the acoustic performance of the cloak. Through expanding into the non-gradient and disorder cases, wider-band cloak with better cloaking feature can be realized through data-driven multi-scale inverse design. Besides, existing works were restricted to 2D or 3D domains created by the rotational symmetric 2D structure. Eventually, fully 3D inverse design can create an acoustic cloak that can eliminate all-angle scattering in a stereoscopic space. Meanwhile, design of unwater acoustic cloak calls for the consideration of acoustic-structure coupling.

Low-frequency vibration/sound suppression

Another important aspect that relates to the wave propagation properties of phononic metamaterials is the low-frequency vibration suppression [82], sound insulation, and perfect absorption, which have been difficult to achieve using conventional materials/structures. Unlike the optimization of effective parameters in Section of "Negative effective properties", similar double-negative acoustic metamaterials can be optimized by minimizing the amplitude of the sound pressure gradient in solids [122,262]. In recent years, data-driven and physics-informed machine learning algorithms have been used for the inverse design of phononic metamaterials. For example, using the generative adversarial network, the designed cavity structures can possess desired sound insulation [172]. Based on physics-informed deep learning, inversely-designed elastic metamaterials containing piezoelectric materials can realize multifunctional wave control without changing microstructures [263]. For elastic metamaterials, combination of local resonances with the surface waves, topology-optimized slim connections and large masses can entail the ultra-low-frequency ultra-broadband bandgaps (1.61–4.08 Hz) for isolating seismic wave [264]. The optimization of sound transmission spectra through probability-density machine learning can derive metamaterials in a high-dimensional parameter space [265]. Similarly, the metamaterials supporting broad-

Please cite this article in press as: H.-W. Dong et al., Materials Today, (2024), https://doi.org/10.1016/j.mattod.2024.09.012

band perfect absorption can be designed by probabilistic generation network [266].

As far as low-frequency vibration suppression is concerned, no study considers the bearing capability during the inverse design and even the effect of long-period vibration on fatigue rupture. As to the low-frequency sound insulation, progress made on bandwidth and low-frequency performance is still insufficient. Overall, the current inverse-designed phononic metamaterials are dependent on the reported mechanisms and configurations. To break the low-frequency and broadband limit, it is possible to leverage factors like nonlinear constitutive relations, amplitude-induced features, semi-active/active controls, and other nonlinear factors into the inverse design model. Meanwhile, 3D modelling and consideration can further enhance the low-frequency vibration and sound suppression.

Extreme-mode-enabled propagation

In addition to the aforementioned applications, other approaches leverage propagation properties such as strong anisotropy and extreme wave modes by controlling the dispersion relations. For example, when the band structures combined with the eigenfrequency curves were optimized, non-resonant broadband hyperbolic elastic metamaterials can be inversely designed [92], leading to a triangular converter for mode conversion (Fig. 13d) [267]. When the optimization objective was set to minimize the difference between the target modulus matrix and the realistic effective modulus matrix [268–270], it was possible to achieve extreme properties with near-zero shear modulus, water-like bulk modulus and coupling modulus, which can be utilized to construct pentamode stealth cloaks [268]. Similarly, the optimization of all involved effective moduli can enable 3D solid pentamode micro-lattices that can be fabricated by the additive manufacturing technique of selective laser melting (Fig. 13d) [68]. A strong anisotropy through the customized longitudinal, transverse, and coupling moduli, on the other hand, leads to perfect transmodal Fabry-Perot interference [271]. Notably, the inverse design of microstructures with zero-energy modes based on the directed-graph theory can enable anomalous dispersion cones that nucleate from extreme spatial dispersion at 0 Hz (Fig. 13d), which breaks the cognition of physical principle for metamaterials [272]. Moreover, other advanced, user-customized functionalities have also been realized with the help of inverse design. For example, analog computing was demonstrated by judiciously controlling the wave signals via inversely designed scatterers [273].

The above studies indicated that more fancy wave modes can be explored through leveraging anisotropy and non-local effects. Nevertheless, existing researches mainly focused on the single-phase or two-phase materials. Should three-phase or multiple-phase materials be considered, especially the combination of hard and soft constituents, more complex and exotic wave modes can be captured with the help of inverse design. Furthermore, if nonlinear (large deformation) or micro-mechanism structure is involved, it is possible to discover more proteiform modes through inverse design of a coupled mechanism-structure system. Besides, existing studies are limited to the 2D cases. If the design domain is extended to the 3D space, it is very promising to find out more extreme modes through inverse design, thus contributing to novel applications through the wave mode control [106].

Phononic metasurfaces

Inverse design of phononic metasurfaces requires elaborate tailoring of the microstructures and their ordering, in either passive and active manners, to achieve specific phase, amplitude, and polarization combinations. Controlling these characteristic quantities allows for the flexible control of the wavefront for realizing exotic phenomena related to reflection, refraction, focusing, cloaking, illusion, vortex beams, and so on. During the last 10 years, a series of customized phononic metasurfaces were inversely designed through optimizing diverse wave scattering, i.e., phase, amplitude, and impedance, for the reflective, absorptive, transmissive, and even multifunctional elastic or acoustic functionalities, as shown in Fig. 14.

Abnormal reflection and absorption

Up to now, most inversely designed phononic metasurfaces were obtained based on the Generalized Snell's law [274]. Based on the SIMP, transfer matrix method containing the mean finite-element results can bring abnormal reflection and even 90-degree reflected longitudinal waves [275] (Fig. 14a). Based on the manipulation of reflective energy flux, maximizing the specific-order diffraction efficiency can achieve waterborne metagrating with high-efficiency anomalous reflection, thus realizing perfect beam splitting and highly asymmetric transmission response [276]. Utilizing a similar inverse-design strategy, one can design abnormal deflection with near-perfect efficiency of elastic longitudinal and transverse waves [277]. With the help of machine learning, parameter optimizations of non-local acoustic metasurfaces [278] (Fig. 14a) or metagrating with Willis coupling [153] can effectively generate efficient abnormal reflection with a prescribed diffraction order. Using the inverse design based on the grating diffraction theory, optimizing the real and imaginary parts of the reflection phase of every unit can produce high-efficiency abnormal reflection [279]. In another study, the surface impedance theory [65] determines the required surface impedance which correlates with the reflection phase. Then the targeted units or the entire supercell can be designed through local [280] or non-local patterns.

In contrast to phase manipulation, the amplitude encodes the elastic or acoustic wave intensity information that is useful to realize functions like sound absorption, insulation, and gain, etc. For example, in an acoustic-elastic coupling system, the maximization of shear wave amplitude in the elastic region can entail the conversion from airborne sound waves to transverse waves [281]. By minimizing the loudness based on Zwicker's model, inverse design of the difunctional metasurfaces supporting the sound insulation and ventilation was also made possible [128]. When machine learning was applied to labyrinth-resonance metasurface design, perfect low-frequency airborne sound absorption can be achieved [173,202]. Using an ultrasparse dissipated-sound metacage (Fig. 14a), the maximization of absorption efficiency at a prescribed frequency leads to an omnidirectional suppression of acoustic radiation [208] (Fig. 14a).

Aforementioned phononic reflective and absorptive metasurfaces are crucial to airborne noise control and underwater acous-

Please cite this article in press as: H.-W. Dong et al., Materials Today, (2024), https://doi.org/10.1016/j.mattod.2024.09.012

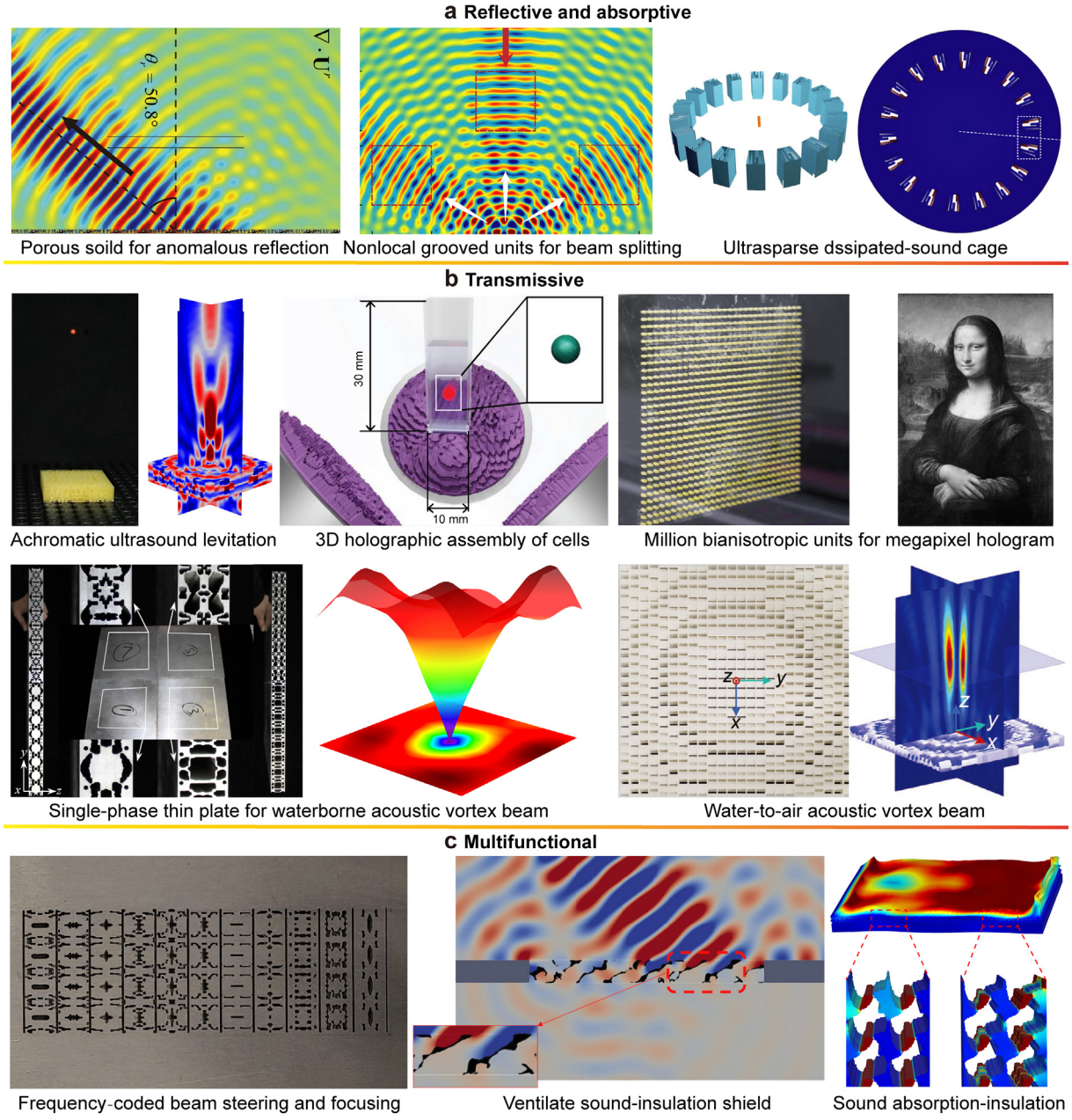

FIG. 14

Inverse-designed phononic metasurfaces. (a) Elastic gradient metasurface, nonlocal acoustic metasurface, and ultrasparse metacage for abnormal reflection/absorption. Reproduced with permission from Refs. [208,275,278]. (b) Acoustic metasurface with customized transmissive wavefronts for ultra-broadband ultrasound levitation, 3D holographic assembly, megapixel hologram, underwater/water-to- air acoustic vortex beams. Reproduced with permission from Refs. [52,53,283–285]. (c) Multifunctional metasurfaces for two kinds of elastic beams, integrated sound insulation-ventilating and underwater absorption-insulation. Reproduced with permission from Refs. [85,129,201].

tic stealth. However, current research can hardly cope with some key engineering constraints/factors during inverse design, e.g., the compatibility of lightweight with acoustic functionality, effect of aerodynamic environment, impact of extreme temperature or wide temperature variation, and implications of hydrostatic pressure on the load-bearing capability of the design structures without compromising acoustic performance, etc. Besides, most of the existing inverse-designed phononic metasurfaces are passive. The deployment of smart materials, sensing and control techniques maybe an effective strategy for intelligent phononic metasurface design.

Transmissive and force-trapping beams

For transmissive wavefront engineering, the inverse-design scheme synthesizing the phase-dispersion-functionality can generate a series of novel asymmetric metasurfaces for ultra-broadband achromatic negative refraction and focusing. The mechanism underlying the ultra-broadband achromatic nature was shown to originate from the integration of internal resonances, bi-anisotropy, and multiple scattering [52]. When broadband non-linear dispersion was considered, the combination of a 2-bit strategy and constant phase difference can give rise to airborne acoustic diffusion scattering [83]. With chiral phase distri-

Please cite this article in press as: H.-W. Dong et al., Materials Today, (2024), https://doi.org/10.1016/j.mattod.2024.09.012

bution, broadband high-efficiency airborne acoustic vortex beam can be inversely designed [282]. Should the acoustic-structure coupling in the underwater environment is involved, inverse-designed coding metasurfaces can realize waterborne acoustic vortex beam [283] (Fig. 14b). In the air–water interface, the hybrid metasurfaces can realize the water–air-cross plane-vortex transmission [284] (Fig. 14b). Based on the manipulation of transmissive energy flux, combined with the dual-scale homogenization method, maximizing the acoustic wave energy in the target region and minimizing the energy in the other domain can enable high-efficiency negative refraction with a prescribed refraction angle [146].

Controlling the entire wave field based on phase manipulation can give rise to acoustic holograms, which can be used for levitation and acoustic tweezers through a meticulous manipulation of the radiation force. For instance, depending on the targeted holography image, optimizations can lead to acoustic metasurfaces encoding phase information for airborne or waterborne holographic imaging and particle trapping [16], and 3D holographic assembly of cells and microgel beads [285] (Fig. 14b). As for obtaining the precise acoustic radiation force within a broadband range, an inversely-design achromatic acoustic metasurface with customized dispersions can give rise to stable and single-sided ultrasound levitation [52] (Fig. 14b). To solve the low-resolution problem behind the metasurface-based holography, a deep-learning-enabled universal inverse-design platform for acoustic metasurfaces with millions of microstructures was proposed based on the Huygens-Fresnel principle to realize four-megapixel acoustic hologram by utilizing the iterative compensation optimization method [53] (Fig. 14b).

Despite the encouraging progress made on transmissive and force-trapping beams, some key problems remain to be solved in relation to their inverse design. For instance, existing inverse design mainly focuses on the constructions of local metasurface elements and their assembly. Most studies only adopt weak coupling assumption or hard boundary treatment to ignore the coupling between adjacent elements. A more systemic and effective approach is to conduct the inverse design of non-local models. In addition, no studies take full advantages of the loss manipulation. The non-local inverse design with proper consideration of loss in the system is expected to enhance the transmission efficiency. For underwater transmissive metasurfaces, current inverse design only considers the acoustic-structure coupling instead of fluid–structure-acoustic coupling. It is of anticipated interest and challenging to inversely design the underwater acoustic metasurfaces under flow. As for force-trapping beams, the resulting acoustic radiation force is easily affected by phase deviation. To construct an ideal force-trapping beam, it is necessary to design the metasurface with the targeted radiation force by end-to-end optimization.

Multifunctional scattering

Considering frequency-dependent phase features, multiple-functional elastic metasurfaces can be designed for the frequency-coding mixing elastic wave functionalities [201,286] (Fig. 14c). Similarly, the minimization of the square averaged pressure of the object region can enable bi-functional broadband multi-angle sound insulation and ventilation [129] (Fig. 14c). Unlike the design based on phase and amplitude, tailoring the polarization vector can also control the multiform elastic or acoustic wave modes by a metasurface. In theory, wave mode conversions can be exploited for enhanced sound absorption, insulation, and filtering, etc. Taking the underwater acoustic metaconverters as an example, the inverse design of effective moduli can create specific polarization to support the multiple transmissive and reflective longitudinal–transverse wave conversion, which contributes to the broadband efficient underwater sound absorption and insulation simultaneously [84,85] (Fig. 14c). Based on a multilayer perceptual network model, it is possible to design an elastic metasurface with focusing and abnormal refraction at different frequencies through optimizing the real and imaginary parts of the transmission coefficient [157].

Although some multifunctional metasurfaces have been proposed, the inverse-designed metasurfaces are limited to the simple combination of two functions or two kinds of beams. No inverse design from the perspective of multi-objective optimization is available to balance two or more functions. What is more critical is how to characterize the multiphysics fields and trade-offs in the inverse design according to the requirements of practical applications.

Applications of customized PMSMs

Despite the rapid development of PMSMs which demonstrates the fascinating wave phenomena and understanding of fundamental physics, real-world applications of PMSMs are largely insufficient, despite several attempts being made. We are about to enter an era where the practical implications of the concept need to be demonstrated through real-life examples and brought closer to future engineering implementations. In this regard, compared to traditional or empirical design, the inverse-design strategy offers an efficient means for structural design. In addition to achieving better performance in terms of wave manipulation with the consideration of rigorous objective parameters, multiple constraints involved, manufacturing limitations, etc, practical constraints can also be embedded into the design framework in a more flexible manner. Recent works have documented several practical applications of inversely customized PMSMs including nondestructive testing or structural health monitoring (SHM) [243,287], sound absorption [238,288], energy harvesting [289], and high-resolution holograms [16], see Fig. 15.

As a representative example, the use of metamaterials in SHM has shown great promise for modulating the probing signals and enhancing the detection accuracy of incipient damage/defects in engineering structures. To cope with the specific needs of nonlinear guided wave-based detection methods [290,291], inverse-design method allows for the development of tailor-made metamaterials under the harsh requirements imposed by the SHM including maintaining the integrity of the structure under inspection while ensuring SHM-desired functions [292]. More specifically, an inverse-designed meta-filter was introduced as an add-on device to the structure under inspection to facilitate the implementation of nonlinear-guided-wave-based SHM technique through the manipulation of the probing waves. Inverse-designed metamaterial devices were deployed to fulfill three major SHM-specific functions: wave filtering [243], steering and mode conversion [287]. An example is shown in Fig. 15a,

Please cite this article in press as: H.-W. Dong et al., Materials Today, (2024), https://doi.org/10.1016/j.mattod.2024.09.012

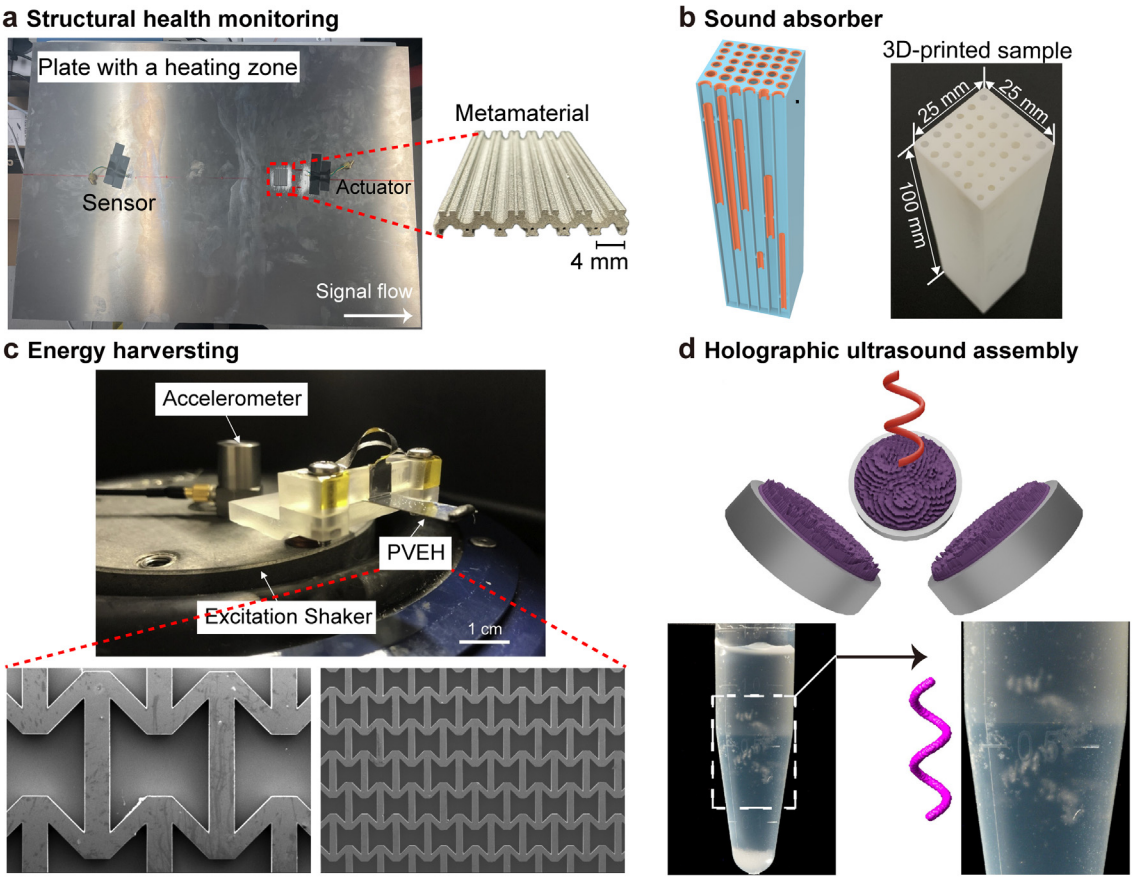

FIG. 15

Representative applications brought by inverse-designed PMSMs with customized functionalities. (a) Add-on meta-filter for nonlinear-guided-wave-based structural health monitoring. Reproduced with permission from Ref. [287]. (b) Non-local sound metamaterial absorber for optimal low-frequency broadband near-perfect absorption. Reproduced with permission from Ref. [288]. (c) Metamaterial-based vibration energy harvesters for high power collection. Reproduced with permission from Ref. [289]. (d) Rapid on-step 3D assembly of silica gel beads with holographic ultrasound fields using three acoustic metasurfaces. Reproduced with permission from Ref. [285].

illustrating an inversely customized metamaterial device [287], attached on the surface of a plate under inspection, to achieve high-efficiency antisymmetric-to-symmetric mode conversion, since the latter is more conducive to the generation of the cumulative second harmonics, used as the damage indicator.

Other attempts have also been made regarding diverse wave functionalities of PMSMs. For noise reduction, size optimization was utilized to design a metamaterial absorber for efficient sound absorption. Results indicated that deploying a non-local 3D-printed absorber, the average absorption coefficient can reach 93 % in the range of 320–6400 Hz [288], see Fig. 15b. Another example is a vibration energy harvester, shown in Fig. 15c [289], which were designed by systematically adjusting the dimensions of the metamaterial structure for their elastic layers. The proposed designs achieved high power harvesting with reduced structural size, which might potentially serve as the power source for the Internet of Things in the future. In addition, to achieve 3D assembly of particles using the acoustic hologram, a systematic design strategy was developed to conduct meticulous customization for achieving the desired acoustic phase or amplitude distribution [285], see Fig. 15d. These studies demonstrate the feasibility of applying inverse-designed PMSMs to tackle potential applications. It goes without saying that the specific functions that a PMSM needs to deliver are mission-driven that should come from the domain knowledge of the related physics and engineering field. Importantly, inverse-design provides a powerful tool for the task. This having said, the technique is still at an early development stage, and deserves further research efforts considering its potential value and practical significance. It is envisioned that the power offered by the inverse design will lead to a wider range of practical applications, unlocking the potential of PMSM from an application perspective.

Outlook and summary

Outlook

We point out the following aspects as directions for future efforts to achieve more robust acoustic and elastic wave control in the context of PMSM development. Addressing these open issues will help enable the next generation of inverse-engineered PMSMs to meet the functionality and smart wave control capabilities required by users.

Please cite this article in press as: H.-W. Dong et al., Materials Today, (2024), https://doi.org/10.1016/j.mattod.2024.09.012

New techniques

- **High-order dynamic homogenization.** The commonly used dynamic homogenization methods usually adopt the strategy of calculating the boundary stresses or reactions under an applied intrinsic strain field and retrieving the effective parameters through the low-frequency dispersion relation or scattering matrix. However, the adopted homogenization methods are based on the traditional continuum theory, which ignores complex local resonances and rotational motion, thus resulting in inaccurate estimation of effective parameters. This limits the current inverse design to high-symmetry assumptions such as square, chiral and orthogonal symmetries, etc. For relaxing the topological constraint, it is crucial to develop a generalized high-order dynamic homogenization scheme. Subsequently, the effective mass density will become a second-order tensor, while the effective modulus matrix can be asymmetric [293]. Similarly, the improved dynamic homogenization is needed to consider the Willis coupling for the Willis media. In addition, the existing dynamic homogenizations are limited to the very small wavevector ($\mathbf{k}\approx 0$). A generalized homogenization is required to characterize both the large wavevector and high-frequency range. Effective utilization of this new homogenization can significantly expand the design space and offer more possibilities for the exploration of exotic wave properties.
- **Large-scale inverse design.** The application of PMSMs in real-world environments often requires a large number of microstructures or elements to achieve optimal performance. This brings about both challenges and opportunities for large-scale inverse design. For example, the giga-voxel-based computational morphogenesis combined with a parallel implementation of the moving asymptote approach can produce optimal full-size aircraft wing with unprecedented structural resolution [111]. On the other hand, classic surrogate models or fuzzy theories incorporating machine learning are also promising candidates for large-scale inverse design of PMSMs. It is worth noting that the designed large-scale structure may inevitably comprise some complex local components. How to appropriately simplify the structure to extract the beneficial topological features will be of great significance.
- **Multi-scale inverse design.** Inspired by the multi-scale structures in nature [119], multi-scale PMSMs can further expand the design space while maintaining a delicate balance of load-carrying capacity, wave function, and mechanical properties, and so on. However, the vast majority of inverse-designed PMSMs are simply assembled with mesoscopic stackable microstructures lacking intrinsic hierarchies. Therefore, multi-scale PMSMs that consider effects adjacent to or beyond their neighbors using concurrent multi-scale optimization method can, therefore, improve performance and applicability. However, how to accurately conduct homogenization during the design process may be a practical challenge.
- **4D inverse design.** Existing inverse-designed PMSMs are limited to optimizing the microstructural topology and microstructure distributions, without considering any time-term factors. If the spatio-temporal modulated phononics are targeted [294], introducing time related terms into optimization model and considering the non-equilibrium matter under the time-domain periodic modulation can give rise to disruptive PMSMs similar to time crystals [295,296].
- **End-to-end inverse design.** Current inverse design of PMSMs generally requires human intervention to accommodate complex or challenging requirements. For example, when the subwavelength imaging is targeted, a representative inverse design usually adopts ToP or machine learning to generate the phononic metamaterials with negative effective properties. Then the suitable assembly of metamaterial microstructures is used for the resulting subwavelength imaging. In fact, this inverse-design approach reduces the design space and intrinsically introduces the subjective consciousness or experience. Hence, there is a need to develop end-to-end inverse design approaches that directly provides expected PMSM-based devices according to initial targets, avoiding any human intervention and enhancing the design capability.

Emerging areas

- **Multifunctional PMSMs.** Due to the lack of multi-objective optimization models, most inverse-designed PMSMs support only a single function. As such, systematic multi-objective inverse-design models are needed to provide compatibilities among multiple functions. In principle, multi-functional inverse design can be performed for the following cases, namely acoustic multi-functionality (e.g., absorption, insulation, and low-scattering) [297], fusion of acoustic and electromagnetic wave utilities [298], integration of acoustic functionalities with mechanical properties (e.g., sound absorption-insulation and impact-resistance) [299,300], consideration of acoustic functionalities with other constraints (e.g., hydrophobic properties, high-temperature resistance) [301,302], etc. The underlying challenge lies in building a suitable physical multi-objective optimization model and employ appropriate multi-objective optimization algorithms (e.g., NSGA-II, MOPSO, SPEA2, etc.) to obtain the near-optimal multi-objective solution set with good diversity rather than the weighted single-objective optimizations.
- **Reconfigurable PMSMs.** Compared with the passive PMSMs, the PMSMs with controllable components or materials can realize the real-time flexible dynamic control of elastic/acoustic waves, thus greatly enriching the functionalities of PMSMs. When the multiple modes, gradient topology, complex geometric/topology reconstruction are introduced simultaneously, the transformable free-form PMSMs under control is expected to be realized for alterable wave engineering in the future, like the Transformers.
- **Time-varying PMSMs.** Existing PMSM designs are limited to the spatial dimension. However, the time-varying feature can offer an additional degree of freedom to expand the limits of phononic wave control. Thanks to the rapid variation of material parameters or effective parameters, the time-varying PMSMs are expected to authentically break the time reversal invariance, linear-frequency conversion, and non-reciprocal propagation, etc. How to inversely design these brand-new

Please cite this article in press as: H.-W. Dong et al., Materials Today, (2024), https://doi.org/10.1016/j.mattod.2024.09.012

PMSMs will be a very interesting topic. For example, it is promising to combine quantum mechanics and time-varying convex/non-convex optimization.

- **Intelligent PMSMs.** With the rapid development of smart materials and artificial intelligence, intelligent PMSMs are promising and worthy of in-depth research in the future. Unlike existing tunable and reconfigurable PMSMs with active or semi-active control, intelligent PMSMs should have more powerful functions, including perceptive and transforming functions [303] with feedback-control technology, and eventually realize a closed-loop system that combines perception, learning, decision-making, and regulation. However, the inverse design of intelligent PMSMs might involve large deformation, nonlinearity, hard-soft structures, and sophisticated control algorithms. These challenging issues call for more interdisciplinary effort and collaborations. Taking the constitutive relations of smart materials, the topology of structural architectures, and controlling parameters as design variables, the inverse design of PMSMs can enable advanced and intelligent phononic functions, and ultimately a seamless human–machine or environment-machine interface.
- **Non-Hermitian PMSMs.** Most inverse-designed PMSMs behave as a Hermitian system. When the imaginary-part parameters have gain and loss, the inverse-designed PMSMs can be regarded as non-Hermitian systems which would trigger new interesting physical phenomena [107]. If an inverse-design model based on imaginary part parameters or derived parameters is constructed, the generated topologies can give rise to the customized singular points and modes, which can help to achieve functions that are difficult to achieve with Hermitian systems, such as nonreciprocal transmission, perfect absorption, and enhanced sensitivity.

Issues to be addressed

- **Multiphysics.** From a practical application point of view, extreme operating conditions should be considered when inverse designing. In this case, it is necessary to model the PMSM based on multi-physics couplings, such as fluid–solid-acoustic coupling, acousto-hydrodynamic coupling, and opto-mechanical coupling [304], etc. Therefore, it is a long-term challenge to inversely design PMSMs by integrating these multiphysics considerations. Moreover, a noticeable challenge is to develop the advanced multi-objective optimization algorithms for complex multiphysics problems with more than three objectives.
- **Multidisciplinary efforts.** Bringing the proof-of-concept design to the real-world applications requires a systematic and holistic inverse design framework to be endeavored in engineering design in order to integrate multidisciplinary expertise. For example, different disciplines such as acoustics, aeroelasticity, structural vibration, high-temperature mechanics, manufacturing and mechatronics are required to inversely design an aero-engine with a PMSM-based acoustic liner [305,306]. Studying the coupling relationships and constraints between disciplines, solving computational efficiency problems, and incorporating artificial intelligence are important future research topics.
- **Physical principle of novel topologies.** Some recent studies have shown that there are physical bounds that limit a PMSM's property (e.g., causality, Chu's limit, etc.) [28,307]. Deployment of inverse design to reach these properties (e.g., causally optimal absorbers; cloaking devices with theoretically-optimal bandwidth and scattering reduction) is yet to be realized. On the other hand, one can also use these physical principles to inform and guide the design and optimization for better efficiency.
- **High manufacturability.** Inverse-designed PMSMs usually contain unconventional topologies, which place high demands on fabrication. Whether it is single- or multi-phase PMSMs, they usually feature very complex microstructures, nonintuitive ordering structures, zigzag interfaces, complex connections, hollow structures, etc. In addition to fabrication constraints (e.g., maximal/minimal size constraints, closed cavity constraints, overhang constraints, manufacturing defects, and connectivity), the topological complexity of PMSMs needs to be taken into account during the inverse design process.

New possibilities

- **Bio-inspired principle.** For the inverse design of PMSMs, a common problem is the significant impact of initial guess or populations on the generation results and topology, especially for complex wave control using gradient optimization. It is well known that various biological structures in nature contain abundant and subtle scientific principles. If bio-inspired structural features can be introduced in the inverse-design model, the customized wave functionalities can be further improved and even constitutionally comprise a multi-functional nature.
- **Extreme functionalities.** Encouraged by the rapid progress of quantum-mechanics-enabled PMSMs, future inverse-design studies could focus on the extreme functionality by considering extreme wave-matter interactions or confinements (e.g., bound states in the continuum) and quantum-inspired effects (e.g., Klein tunneling, quantum computing).
- **Phononic structures genome engineering (PSGE).** To expand the inverse-design methodology of PMSMs, we proposed the concept of PSGE, in which microstructured microstructure building blocks are used as structure genes, and the ToP and machine learning are used to construct arbitrary multi-hierarchy meta-structured materials with diverse types of structure genes. The process allows for customized phononic wave engineering in which the PMSMs can be realized by the advanced manufacturing technology while the resulting functionalities can be evaluated by the high-precision detecting technology. In brief, PSGE contains four aspects of correlative mechanisms between topology and physics (e.g., intrinsic connections between building blocks/connections/microstructures/ordering structures and elastic/acoustic characteristics), combined data-driven and physics-driven inverse-design theory and method (e.g., integrated structure-functionality design, multi-field and multi-functional design, 4D inverse-design theory and dynamic intelligent control, bio-inspired design), high-performance

Please cite this article in press as: H.-W. Dong et al., Materials Today, (2024), https://doi.org/10.1016/j.mattod.2024.09.012

manufacturing technology (e.g., cross-scale manufacturing using 3D or 4D printing), and advanced detecting technology (e.g., ultrasonic internal inspection and monitoring) for PMSMs. With respect to inverse design of PMSMs, the anticipated approach in PSGE may include three connotations. The first one is a gene pool that encodes the basic properties of irreducible building blocks. This can be inverted by using ToP or machine learning to inversely design rich customized microstructures and classifying them according to scientific principles using generic models. In the second aspect, one can estimate the appropriate combination of building blocks for the interface on demand. For example, if the connections are movable or extremely flexible, machine learning should be favored to guide the assembly of all relevant building blocks according to the suitable growth pattern [308]. The arrangement of the building blocks can be disordered or have nonlinear effects. Finally, after accumulating a large amount of data, a complete model based on PMSMs can be established. This model is expected to provide large-scale and high-efficiency/fidelity evolution of complex PMSM-based systems and enable online customized inverse design of PMSMs for rapid construction and manufacturing. As for the application prospect of PSGE, a representative example is a general-purpose software of PMSMs that integrates analysis, inverse design, and virtual experimentation, which will greatly facilitate the development of PMSM-based technologies.

- **Novel applications.** Inverse design greatly helps the development of novel PMSMs with enhanced and tailor-made functionalities and may lead to more abundant potential applications in the future, such as cell control, underwater detection, information encryption, information operation, intracranial ultrasound imaging, ultrasound medical treatment, low-frequency broadband high-bearing vibration isolators, high-precision vibration identification, transmedia/ultrasound energy harvesting and micromachining, etc. In particular, future studies can leverage the inverse-designed PMSM as a hidden layer for decoding information of the novel artificial intelligence technology. In other words, the elaborated PMSMs can become hardwares for a diffractive deep neural network [309,310].

Through continuous efforts to address the above challenges, the inverse design of PMSMs is expected to play a central role in acoustic/elastic wave engineering and beyond.

Summary

In this Review, we systematically examine the development and the state-of-the-art of PMSM inverse design, including concepts, methods, configurations, and representative applications, and compare them with traditional intuitive design methods. In particular, based on specific physical mechanisms or fundamental wave quantities, the inverse design methodology of PMSMs using ToP and machine learning is elaborated. Then, various realized PMSMs are discussed in terms of extreme wave motions, on-demand wave functionalities, novel topologies, unexplored physical mechanisms, and attractive application perspectives, etc. Finally, future directions and challenges in relation to PMSM inverse design are outlined. This Review is expected to serve as an important guide for the development and practical applications of PMSMs in the near and distant future.

CRediT authorship contribution statement

Hao-Wen Dong: Writing – review & editing, Writing – original draft, Visualization, Validation, Supervision, Project administration, Methodology, Investigation, Conceptualization. **Chen Shen:** Writing – review & editing, Writing – original draft, Supervision, Methodology, Investigation, Conceptualization. **Ze Liu:** Writing – original draft, Resources. **Sheng-Dong Zhao:** Resources, Investigation. **Zhiwen Ren:** Resources, Investigation. **Chen-Xu Liu:** Resources, Investigation. **Xudong He:** Resources, Investigation. **Steven A. Cummer:** Validation, Supervision. **Yue-Sheng Wang:** Writing – review & editing, Supervision, Methodology, Conceptualization. **Daining Fang:** Writing – review & editing, Supervision, Project administration, Conceptualization. **Li Cheng:** Writing – review & editing, Writing – original draft, Supervision, Conceptualization.

Data availability

Data will be made available on request.

Declaration of competing interest

The authors declare that they have no known competing financial interests or personal relationships that could have appeared to influence the work reported in this paper.

Acknowledgments

This work was supported by the National Natural Science Foundation of China (Grant Nos. 52250217, 12172044 and 12021002) and the Beijing Institute of Technology Research Fund Program for Young Scholars.

References

[1] R. Martínez-Sala et al., Nature 378 (6554) (1995) 241. https://doi.org/10.1038/378241a0.
[2] X. Jiang et al., Science 370 (6523) (2020) 1447–1450. https://doi.org/10.1126/science.abe2011.
[3] M. Eichenfield et al., Nature 462 (7269) (2009) 78–82. https://doi.org/10.1038/nature08524.
[4] T.P. Purdy et al., Science 356 (6344) (2017) 1265–1268. https://doi.org/10.1126/science.aag1407.
[5] R.H. Olsson, I. El-Kady, Meas. Sci. Technol. 20 (1) (2009) 012002. https://doi.org/10.1088/0957-0233/20/1/012002.
[6] Y. Pennec et al., Surf. Sci. Rep. 65 (8) (2010) 229–291. https://doi.org/10.1016/j.surfrep.2010.08.002.
[7] T.G. Lee et al., Nano Energy 78 (2020) 105226. https://doi.org/10.1016/j.nanoen.2020.105226.
[8] C. He et al., Nat. Phys. 12 (12) (2016) 1124–1129. https://doi.org/10.1038/nphys3867.
[9] J. Cha et al., Nature 564 (7735) (2018) 229–233. https://doi.org/10.1038/s41586-018-0764-0.
[10] H.L. He et al., Nature 560 (7716) (2018) 61–64. https://doi.org/10.1038/s41586-018-0367-9.
[11] Z.Y. Liu et al., Science 289 (5485) (2000) 1734–1736. https://doi.org/10.1126/science.289.5485.1734.
[12] L. Zigoneanu et al., Nat. Mater. 13 (4) (2014) 352–355. https://doi.org/10.1038/nmat3901.
[13] S. Zanotto et al., Nat. Commun. 13 (1) (2022) 5939. https://doi.org/10.1038/s41467-022-33652-8.
[14] J. Xu et al., Nat Commun 14 (1) (2023) 869. https://doi.org/10.1038/s41467-023-36581-2.

Please cite this article in press as: H.-W. Dong et al., Materials Today, (2024), https://doi.org/10.1016/j.mattod.2024.09.012

[15] Y.B. Xie et al., Nat. Commun. 5 (2014) 5553. https://doi.org/10.1038/ncomms6553.
[16] K. Melde et al., Nature 537 (7621) (2016) 518–522. https://doi.org/10.1038/nature19755.
[17] F. Li et al., Phys. Rev. Appl. 13 (4) (2020) 044077. https://doi.org/10.1103/PhysRevApplied.13.044077.
[18] M. Caleap, B.W. Drinkwater, Proc. Natl. Acad. Sci. U. S. A. 111 (17) (2014) 6226–6230. https://doi.org/10.1073/pnas.1323048111.
[19] S.J. Yang et al., Nat. Mater. 21 (5) (2022) 540–546. https://doi.org/10.1038/s41563-022-01210-8.
[20] G.M. Della Pepa et al., Neurosurg. Focus 50 (1) (2021) 11 E15. https://doi.org/10.3171/2020.10.Focus20797.
[21] Y. Achaoui et al., Extreme Mech. Lett. 8 (2016) 30–37. https://doi.org/10.1016/j.eml.2016.02.004.
[22] Y.G. Peng et al., Nat. Commun. 7 (2016) 13368. https://doi.org/10.1038/ncomms13368.
[23] H.X. Li et al., Research 2019 (2019) 8345683. https://doi.org/10.34133/2019/8345683.
[24] K.J. Ma et al., Sci. Adv. 8 (39) (2022) eadc9230. https://doi.org/10.1126/sciadv.adc9230.
[25] C.X. Hou et al., Commun. Phys. 6 (1) (2023) 252. https://doi.org/10.1038/s42005-023-01361-3.
[26] H.J. Kim et al., Int. J. Mech. Sci. 251 (2023) 108354. https://doi.org/10.1016/j.ijmecsci.2023.108354.
[27] S.C. Qu et al., Build. Environ. 244 (2023) 110753. https://doi.org/10.1016/j.buildenv.2023.110753.
[28] M. Yang, P. Sheng, Appl. Phys. Lett. 122 (26) (2023) 260504. https://doi.org/10.1063/5.0147941.
[29] D.J. Mead, J. Sound Vib. 27 (2) (1973) 235–260. https://doi.org/10.1016/0022-460x(73)90064-3.
[30] J.D. Achenbach, M. Kitahara, J. Acoust. Soc. Am. 81 (3) (1987) 595–598. https://doi.org/10.1121/1.394825.
[31] M.M. Sigalas, E.N. Economou, J. Sound Vib. 158 (2) (1992) 377–382. https://doi.org/10.1016/0022-460x(92)90059-7.
[32] M.S. Kushwaha et al., Phys. Rev. Lett. 71 (13) (1993) 2022–2025. https://doi.org/10.1103/PhysRevLett.71.2022.
[33] S.X. Yang et al., Phys. Rev. Lett. 93 (2) (2004) 024301. https://doi.org/10.1103/PhysRevLett.93.024301.
[34] , Springer, Berlin, Germany, 2015, pp. 971–978.
[35] S.A. Cummer et al., Nat. Rev. Mater. 1 (3) (2016) 16001. https://doi.org/10.1038/natrevmats.2016.1.
[36] G.C. Ma et al., Nat. Mater. 13 (9) (2014) 873–878. https://doi.org/10.1038/nmat3994.
[37] B. Assouar et al., Nat. Rev. Mater. 3 (12) (2018) 460–472. https://doi.org/10.1038/s41578-018-0061-4.
[38] G.C. Ma, P. Sheng, Sci. Adv. 2 (2) (2016) e1501595. https://doi.org/10.1126/sciadv.1501595.
[39] E.Q. Dong et al., Natl. Sci. Rev. 10 (6) (2023) nwac246. https://doi.org/10.1093/nsr/nwac246.
[40] J.W. Guo et al., Mater. Today 66 (2023) 321–338. https://doi.org/10.1016/j.mattod.2023.04.004.
[41] M. Oudich et al., Adv. Funct. Mater. 33 (2) (2023) 2206309. https://doi.org/10.1002/adfm.202206309.
[42] T. Vasileiadis et al., J. Appl. Phys. 129 (16) (2021) 160901. https://doi.org/10.1063/5.0042337.
[43] S.C. Qu, P. Sheng, Phys. Rev. Appl. 17 (4) (2022) 047001. https://doi.org/10.1103/PhysRevApplied.17.047001.
[44] J. Mei et al., Nat. Commun. 3 (2012) 756. https://doi.org/10.1038/ncomms1758.
[45] Z. Yang et al., Phys. Rev. Lett. 101 (20) (2008) 204301. https://doi.org/10.1103/PhysRevLett.101.204301.
[46] C.J. Rupp et al., Struct. Multidiscip. Optim. 34 (2) (2007) 111–121. https://doi.org/10.1007/s00158-006-0076-0.
[47] M. Miniaci et al., Phys. Rev. Lett. 118 (21) (2017) 214301. https://doi.org/10.1103/PhysRevLett.118.214301.
[48] R. Lucklum, N. Mukhin, J. Appl. Phys. 130 (2) (2021) 024508. https://doi.org/10.1063/5.0046847.
[49] H. Imanian et al., Sens. Actuator B-Chem. 345 (2021) 130418. https://doi.org/10.1016/j.snb.2021.130418.
[50] Advances in Crystals and Elastic Metamaterials, Pt 2 52 (2019) 105–-145.
[51] O. Sigmund, J.S. Jensen, Philos. Trans. R. Soc. A-Math. Phys. Eng. Sci. 361 (1806) (2003) 1001–1019. https://doi.org/10.1098/rsta.2003.1177.
[52] H.W. Dong et al., Natl. Sci. Rev. 9 (12) (2022) nwac030. https://doi.org/10.1093/nsr/nwac030.
[53] X.B. Miao et al., Appl. Phys. Rev. 10 (2) (2023) 021411. https://doi.org/10.1063/5.0136802.
[54] H.W. Dong et al., J. Mech. Phys. Solids 105 (2017) 54–80. https://doi.org/10.1016/j.jmps.2017.04.009.
[55] R.E. Christiansen et al., Phys. Rev. Lett. 122 (23) (2019) 234502. https://doi.org/10.1103/PhysRevLett.122.234502.
[56] L. Sanchis et al., Phys. Rev. Lett. 110 (12) (2013) 124301. https://doi.org/10.1103/PhysRevLett.110.124301.
[57] A. Dalklint et al., J. Mech. Phys. Solids 163 (2022) 104849. https://doi.org/10.1016/j.jmps.2022.104849.
[58] S.S. Nanthakumar et al., J. Mech. Phys. Solids 125 (2019) 550–571. https://doi.org/10.1016/j.jmps.2019.01.009.
[59] M.H. Lu et al., Mater. Today 12 (12) (2009) 34–42. https://doi.org/10.1016/s1369-7021(09)70315-3.
[60] Y.F. Wang et al., Appl. Mech. Rev. 72 (4) (2020) 040801. https://doi.org/10.1115/1.4046222.
[61] M.I. Hussein et al., Appl. Mech. Rev. 66 (4) (2014) 040802. https://doi.org/10.1115/1.4026911.
[62] G.L. Yi, B.D. Youn, Struct. Multidiscip. Optim. 54 (5) (2016) 1315–1344. https://doi.org/10.1007/s00158-016-1520-4.
[63] G.C. Ma et al., Proc. Natl. Acad. Sci. U. S. A. 115 (26) (2018) 6638–6643. https://doi.org/10.1073/pnas.1801175115.
[64] H.K. Zhang et al., Nat. Commun. 15 (1) (2024) 1270. https://doi.org/10.1038/s41467-024-45435-4.
[65] J.F. Li et al., Nat. Commun. 9 (2018) 1342. https://doi.org/10.1038/s41467-018-03778-9.
[66] Z.L. Du et al., J. Mech. Phys. Solids 135 (2020) 103784. https://doi.org/10.1016/j.jmps.2019.103784.
[67] H.W. Dong et al., J. Opt. Soc. Am. B-Opt. Phys. 31 (12) (2014) 2946–2955. https://doi.org/10.1364/josab.31.002946.
[68] S.H. Wu et al., Comput. Meth. Appl. Mech. Eng. 377 (2021) 113708. https://doi.org/10.1016/j.cma.2021.113708.
[69] Y.F. Chen et al., J. Sound Vib. 410 (2017) 103–123. https://doi.org/10.1016/j.jsv.2017.08.015.
[70] J.J. He, Z. Kang, Ultrasonics 82 (2018) 1–10. https://doi.org/10.1016/j.ultras.2017.07.006.
[71] M.I. Hussein et al., Struct. Multidiscip. Optim. 31 (1) (2006) 60–75. https://doi.org/10.1007/s00158-005-0555-8.
[72] X.P. Zhang et al., Int. J. Mech. Sci. 212 (2021) 106829. https://doi.org/10.1016/j.ijmecsci.2021.106829.
[73] H.W. Dong et al., Ultrasonics 76 (2017) 109–124. https://doi.org/10.1016/j.ultras.2016.12.018.
[74] A. Kazemi et al., Phys. Rev. Lett. 131 (17) (2023) 176101. https://doi.org/10.1103/PhysRevLett.131.176101.
[75] J.H. Park et al., Struct. Multidiscip. Optim. 51 (6) (2015) 1199–1209. https://doi.org/10.1007/s00158-014-1206-8.
[76] Y.F. Li et al., Sci. Rep. 7 (2017) 7445. https://doi.org/10.1038/s41598-017-07914-1.
[77] E. Andreassen et al., J. Sound Vib. 379 (2016) 53–70. https://doi.org/10.1016/j.jsv.2016.03.002.
[78] H.W. Dong et al., J. Sound Vib. 493 (2021) 115687. https://doi.org/10.1016/j.jsv.2020.115687.
[79] Y.F. Chen et al., Mech. Syst. Signal Proc. 146 (2021) 107054. https://doi.org/10.1016/j.ymssp.2020.107054.
[80] R.E. Christiansen, O. Sigmund, Struct. Multidiscip. Optim. 54 (3) (2016) 469–482. https://doi.org/10.1007/s00158-016-1411-8.
[81] K. Matsushima et al., Struct. Multidiscip. Optim. 63 (1) (2021) 231–243. https://doi.org/10.1007/s00158-020-02689-y.
[82] T. Matsuki et al., Appl. Phys. Lett. 104 (19) (2014) 191905. https://doi.org/10.1063/1.4878259.
[83] S.D. Zhao et al., Phys. Rev. Appl. 17 (3) (2022) 034019. https://doi.org/10.1103/PhysRevApplied.17.034019.
[84] H.W. Dong et al., Phys. Rev. Appl. 17 (4) (2022) 044013. https://doi.org/10.1103/PhysRevApplied.17.044013.
[85] H.W. Dong et al., Phys. Rev. Appl. 19 (4) (2023) 044074. https://doi.org/10.1103/PhysRevApplied.19.044074.
[86] H.D. Huynh et al., Extreme Mech. Lett. 61 (2023) 101981. https://doi.org/10.1016/j.eml.2023.101981.
[87] Y. Wu et al., Phys. Rev. B 76 (20) (2007) 205313. https://doi.org/10.1103/PhysRevB.76.205313.

Please cite this article in press as: H.-W. Dong et al., Materials Today, (2024), https://doi.org/10.1016/j.mattod.2024.09.012

[88] B.I. Popa, S.A. Cummer, Phys. Rev. B 80 (17) (2009) 174303. https://doi.org/10.1103/PhysRevB.80.174303.
[89] C. Shen et al., Phys. Rev. Lett. 115 (25) (2015) 254301. https://doi.org/10.1103/PhysRevLett.115.254301.
[90] J.H. Oh et al., Struct. Multidiscip. Optim. 52 (6) (2015) 1023–1040. https://doi.org/10.1007/s00158-015-1288-y.
[91] J.H. Oh et al., Appl. Phys. Lett. 104 (7) (2014) 073503. https://doi.org/10.1063/1.4865907.
[92] J.J. Rong, W.J. Ye, Comput. Meth. Appl. Mech. Eng. 344 (2019) 819–836. https://doi.org/10.1016/j.cma.2018.10.034.
[93] R. Zhu et al., J. Acoust. Soc. Am. 139 (6) (2016) 3302–3309. https://doi.org/10.1121/1.4950728.
[94] N. Fang et al., Nat. Mater. 5 (6) (2006) 452–456. https://doi.org/10.1038/nmat1644.
[95] S. Zhang et al., Phys. Rev. Lett. 106 (2) (2011) 024301. https://doi.org/10.1103/PhysRevLett.106.024301.
[96] Y.Q. Ding et al., Phys. Rev. Lett. 99 (9) (2007) 093904. https://doi.org/10.1103/PhysRevLett.99.093904.
[97] T. Brunet et al., Nat. Mater. 14 (4) (2015) 384–388. https://doi.org/10.1038/nmat4164.
[98] H.W. Dong et al., Acta Mater. 172 (2019) 102–120. https://doi.org/10.1016/j.actamat.2019.04.042.
[99] H.W. Dong et al., J. Mech. Phys. Solids 137 (2020) 103889. https://doi.org/10.1016/j.jmps.2020.103889.
[100] N. Kaina et al., Nature 525 (7567) (2015) 77–81. https://doi.org/10.1038/nature14678.
[101] S.L. Liu et al., Appl. Phys. Lett. 123 (12) (2023) 121701. https://doi.org/10.1063/5.0155865.
[102] A.N. Norris, J. Acoust. Soc. Am. 125 (2) (2009) 839–849. https://doi.org/10.1121/1.3050288.
[103] C.W. Cushing et al., J. Acoust. Soc. Am. 151 (1) (2022) 168–179. https://doi.org/10.1121/10.0009161.
[104] Y. Chen et al., Phys. Rev. B 95 (18) (2017) 180104. https://doi.org/10.1103/PhysRevB.95.180104.
[105] J.M. Kweun et al., Phys. Rev. Lett. 118 (20) (2017) 205901. https://doi.org/10.1103/PhysRevLett.118.205901.
[106] J. Lee et al., Nat. Commun. 15 (1) (2024) 992. https://doi.org/10.1038/s41467-024-45146-w.
[107] L.J. Huang et al., Nat. Rev. Phys. 6 (1) (2024) 11–27. https://doi.org/10.1038/s42254-023-00659-z.
[108] K. Ding et al., Nat. Rev. Phys. 4 (12) (2022) 745–760. https://doi.org/10.1038/s42254-022-00516-5.
[109] Y. Yang et al., Science 383 (6685) (2024) eadf9621. https://doi.org/10.1126/science.adf9621.
[110] M.P. Bendsoe, O. Sigmund, Topology optimization: theory, methods, and applications, Springer Science & Business Media:, 2013.
[111] N. Aage et al., Nature 550 (7674) (2017) 84–86. https://doi.org/10.1038/nature23911.
[112] N. Mohammadi Estakhri et al., Science 363 (6433) (2019) 1333–1338. https://doi.org/10.1126/science.aaw2498.
[113] Y.M. Xie, Architect. Intell. 1 (1) (2022) 2. https://doi.org/10.1007/s44223-022-00003-y.
[114] O. Sigmund, S. Torquato, J. Mech. Phys. Solids 45 (6) (1997) 1037–1067. https://doi.org/10.1016/s0022-5096(96)00114-7.
[115] C.S. Andreasen et al., Int. J. Numer. Methods Fluids 61 (5) (2009) 498–513. https://doi.org/10.1002/fld.1964.
[116] K. Maute, D.M. Frangopol, Comput. Struct. 81 (8–11) (2003) 813–824. https://doi.org/10.1016/s0045-7949(03)00008-7.
[117] J.B. Du, N. Olhoff, Struct. Multidiscip. Optim. 33 (4–5) (2007) 305–321. https://doi.org/10.1007/s00158-006-0088-9.
[118] D. Mousanezhad et al., Phys. Rev. B 92 (10) (2015) 104304. https://doi.org/10.1103/PhysRevB.92.104304.
[119] J. Wu et al., Struct. Multidiscip. Optim. 63 (3) (2021) 1455–1480. https://doi.org/10.1007/s00158-021-02881-8.
[120] M. Nomura et al., Phys. Rev. B 91 (20) (2015) 205422. https://doi.org/10.1103/PhysRevB.91.205422.
[121] X. Liang, J.B. Du, Struct. Multidiscip. Optim. 61 (3) (2020) 943–962. https://doi.org/10.1007/s00158-020-02489-4.
[122] Y. Noguchi et al., Mater. Des. 219 (2022) 110832. https://doi.org/10.1016/j.matdes.2022.110832.
[123] R.E. Christiansen et al., Phys. Rev. Lett. 122 (23) (2019) 6 234502. https://doi.org/10.1103/PhysRevLett.122.234502.
[124] R.E. Christiansen, O. Sigmund, Appl. Phys. Lett. 109 (10) (2016) 101905. https://doi.org/10.1063/1.4962441.
[125] A.R. Gersborg, O. Sigmund, Int. J. Numer. Methods Eng. 87 (9) (2011) 822–843. https://doi.org/10.1002/nme.3133.
[126] G. Fujii et al., Appl. Phys. Lett. 118 (10) (2021) 101102. https://doi.org/10.1063/5.0040911.
[127] V. Cool et al., J. Sound Vib. 568 (2024) 117959. https://doi.org/10.1016/j.jsv.2023.117959.
[128] K. Miyata et al., Comput. Meth. Appl. Mech. Eng. 331 (2018) 116–137. https://doi.org/10.1016/j.cma.2017.11.017.
[129] H. Emoto et al., J. Sound Vib. 567 (2023) 117939. https://doi.org/10.1016/j.jsv.2023.117939.
[130] Z.H. Tian et al., Nat. Commun. 11 (1) (2020) 762. https://doi.org/10.1038/s41467-020-14553-0.
[131] R. Gurunathan et al., Phys. Rev. Mater. 7 (2) (2023) 023803. https://doi.org/10.1103/PhysRevMaterials.7.023803.
[132] Y.Q. Liu et al., Phys. Rev. Lett. 119 (3) (2017) 034301. https://doi.org/10.1103/PhysRevLett.119.034301.
[133] H.F. Zhu et al., Proc. Natl. Acad. Sci. U. S. A. 117 (42) (2020) 26099–26108. https://doi.org/10.1073/pnas.2004753117.
[134] H.W. Dong et al., AIP Adv. 5 (11) (2015) 117149. https://doi.org/10.1063/1.4936640.
[135] Y. Lu et al., Sci. Rep. 7 (2017) 43407. https://doi.org/10.1038/srep43407.
[136] H.W. Dong et al., IEEE Photonics J. 9 (2) (2017) 4700116. https://doi.org/10.1109/jphot.2017.2665700.
[137] G.J. Chaplain et al., Phys. Rev. Appl. 19 (4) (2023) 044061. https://doi.org/10.1103/PhysRevApplied.19.044061.
[138] H.W. Dong et al., J. Mech. Phys. Solids 152 (2021) 104407. https://doi.org/10.1016/j.jmps.2021.104407.
[139] W.Q. Wang et al., J. Appl. Phys. 120 (19) (2016) 195103. https://doi.org/10.1063/1.4967738.
[140] J.R. Willis, Proc. R. Soc. A-Math. Phys. Eng. Sci. 467 (2131) (2011) 1865–1879. https://doi.org/10.1098/rspa.2010.0620.
[141] P. Liu et al., Addit. Manuf. 36 (2020) 101427. https://doi.org/10.1016/j.addma.2020.101427.
[142] W.M. Wang et al., Struct. Multidiscip. Optim. 61 (1) (2020) 1–18. https://doi.org/10.1007/s00158-019-02420-6.
[143] E. Amir, O. Amir, Struct. Multidiscip. Optim. 63 (6) (2021) 2589–2612. https://doi.org/10.1007/s00158-020-02835-6.
[144] W.S. Zhang et al., Struct. Multidiscip. Optim. 56 (3) (2017) 535–552. https://doi.org/10.1007/s00158-017-1736-y.
[145] A. Pizzolato et al., Comput. Meth. Appl. Mech. Eng. 357 (2019) 112552. https://doi.org/10.1016/j.cma.2019.07.021.
[146] Y. Noguchi, T. Yamada, Finite Elem. Anal. Des. 196 (2021) 103606. https://doi.org/10.1016/j.finel.2021.103606.
[147] T. Wu et al., IEEE/CAA J. Autom. Sin. 10 (5) (2023) 1122–1136. https://doi.org/10.1109/jas.2023.123618.
[148] H. Nguyen et al., IET Intell. Transp. Syst. 12 (9) (2018) 998–1004. https://doi.org/10.1049/iet-its.2018.0064.
[149] C. Vermeulen et al., Nature 622 (7984) (2023) 842–849. https://doi.org/10.1038/s41586-023-06615-2.
[150] J. Jumper et al., Nature 596 (7873) (2021) 583–589. https://doi.org/10.1038/s41586-021-03819-2.
[151] H. Feng et al., Nature 627 (8002) (2024) 80–87. https://doi.org/10.1038/s41586-024-07078-9.
[152] W.W. Ahmed et al., Phys. Rev. Res. 3 (1) (2021) 013142. https://doi.org/10.1103/PhysRevResearch.3.013142.
[153] H. Gao et al., Appl. Phys. Lett. 121 (11) (2022) 113501. https://doi.org/10.1063/5.0095217.
[154] Y. Jin et al., Nanophotonics 11 (3) (2022) 439–460. https://doi.org/10.1515/nanoph-2021-0639.
[155] H. Liangshu et al., Microstructures 3 (4) (2023) 2023037. https://doi.org/10.20517/microstructures.2023.29.
[156] C.X. Liu, G.L. Yu, J. Comput. Des. Eng. 10 (2) (2023) 602–614. https://doi.org/10.1093/jcde/qwad013.
[157] W.J. Zhou et al., Mater. Des. 226 (2023) 111560. https://doi.org/10.1016/j.matdes.2022.111560.
[158] S.R.Y. Lee et al., Nano Energy 103 (2022) 107846. https://doi.org/10.1016/j.nanoen.2022.107846.
[159] W. Demeke et al., Extreme Mech. Lett. 65 (2023) 102098. https://doi.org/10.1016/j.eml.2023.102098.

Please cite this article in press as: H.-W. Dong et al., Materials Today, (2024), https://doi.org/10.1016/j.mattod.2024.09.012

[160] H. Baali et al., Commun. Mater. 4 (1) (2023) 40. https://doi.org/10.1038/s43246-023-00369-0.
[161] Z. Zhen et al., Photonics Res. 9 (5) (2021) B229–B235. https://doi.org/10.1364/prj.418445.
[162] H.J. Zhang et al., Acta Mech. Sin. 39 (7) (2023) 9722426. https://doi.org/10.1007/s10409-023-22426-x.
[163] W.J. Miao et al., Chin. Phys. Lett. 40 (1) (2023) 014301. https://doi.org/10.1088/0256-307x/40/1/014301.
[164] Muhammad et al., J. Phys. D-Appl. Phys. 56 (1) (2023) 015106. https://doi.org/10.1088/1361-6463/ac9ce8.
[165] D.H.Y. Lee et al., Int. J. Mech. Sci. 255 (2023) 108474. https://doi.org/10.1016/j.ijmecsci.2023.108474.
[166] T.W. Liu et al., Materials 16 (5) (2023) 1879. https://doi.org/10.3390/ma16051879.
[167] A. Maghami, S.M. Hosseini, Eng. Struct. 263 (2022) 114385. https://doi.org/10.1016/j.engstruct.2022.114385.
[168] D.P. Kingma, M. Welling, 2nd International Conference on Learning Representations, ICLR 2014 – Conference Track Proceedings, International Conference on Learning Representations, ICLR, 2014.
[169] I. Goodfellow et al., Adv. Neural Inf. Process. Syst. 27 (2014) .
[170] C.X. Liu et al., Comput.-Aided Civil Infrastruct. Eng. 39 (5) (2024) 776–790. https://doi.org/10.1111/mice.13100.
[171] Z.H. Wang et al., J. Mech. Des. 144 (4) (2022) 041705. https://doi.org/10.1115/1.4053814.
[172] C. Gurbuz et al., J. Acoust. Soc. Am. 149 (2) (2021) 1162–1174. https://doi.org/10.1121/10.0003501.
[173] K. Donda et al., Extreme Mech. Lett. 56 (2022) 101879. https://doi.org/10.1016/j.eml.2022.101879.
[174] S.H. Han et al., Acta Mech. 234 (10) (2023) 4879–4897. https://doi.org/10.1007/s00707-023-03634-y.
[175] W.F. Jiang et al., Mater. Today Phys. 22 (2022) 100616. https://doi.org/10.1016/j.mtphys.2022.100616.
[176] G.E. Karniadakis et al., Nat. Rev. Phys. 3 (6) (2021) 422–440. https://doi.org/10.1038/s42254-021-00314-5.
[177] Z. Zhang, G.X. Gu, Theoret. Appl. Mech. Lett. 11 (1) (2021) 100220. https://doi.org/10.1016/j.taml.2021.100220.
[178] H. Jeong et al., Comput. Meth. Appl. Mech. Eng. 417 (2023) 116401. https://doi.org/10.1016/j.cma.2023.116401.
[179] C.-X. Liu et al., Int. J. Mech. Sci. 269 (2024) 109080. https://doi.org/10.1016/j.ijmecsci.2024.109080.
[180] Y. Chen et al., Optics Express 28 (8) (2020) 11618–11633. https://doi.org/10.1364/oe.384875.
[181] Y. Tang et al., Nat. Comput. Sci. 2 (3) (2022) 169–178. https://doi.org/10.1038/s43588-022-00215-2.
[182] W. Ji et al., Light-Sci. Appl. 12 (1) (2023) 169. https://doi.org/10.1038/s41377-023-01218-y.
[183] C.-X. Liu, G.-L. Yu, Sci. Rep. 9 (2019) 15322. https://doi.org/10.1038/s41598-019-51662-3.
[184] A. Kadambi et al., Nat. Mach. Intell. 5 (6) (2023) 572–580. https://doi.org/10.1038/s42256-023-00662-0.
[185] Y. Weng, S.G. Paal, Adv. Eng. Inf. 56 (2023) 102000. https://doi.org/10.1016/j.aei.2023.102000.
[186] Z. Chen et al., Nat. Commun. 12 (1) (2021) 6136. https://doi.org/10.1038/s41467-021-26434-1.
[187] H. Chi et al., Comput. Meth. Appl. Mech. Eng. 375 (2021) 112739. https://doi.org/10.1016/j.cma.2019.112739.
[188] W. Ma et al., Adv. Mater. 31 (35) (2019) 1901111. https://doi.org/10.1002/adma.201901111.
[189] M. Li et al., Compos. Struct. 260 (2021) 113254. https://doi.org/10.1016/j.compstruct.2020.113254.
[190] J.F. Li et al., Phys. Rev. Appl. 11 (2) (2019) 024016. https://doi.org/10.1103/PhysRevApplied.11.024016.
[191] G.Y. Su et al., Mech. Syst. Signal Proc. 179 (2022) 109391. https://doi.org/10.1016/j.ymssp.2022.109391.
[192] W. Ma et al., Nat. Photonics 15 (2) (2021) 77–90. https://doi.org/10.1038/s41566-020-0685-y.
[193] S. Molesky et al., Nat. Photonics 12 (11) (2018) 659–670. https://doi.org/10.1038/s41566-018-0246-9.
[194] J.S. Jensen, O. Sigmund, J. Opt. Soc. Am. B-Opt. Phys. 22 (6) (2005) 1191–1198. https://doi.org/10.1364/josab.22.001191.
[195] J.S. Jensen, O. Sigmund, Laser Photon. Rev. 5 (2) (2011) 308–321. https://doi.org/10.1002/lpor.201000014.
[196] O.R. Bilal, M.I. Hussein, Phys. Rev. E 84 (6) (2011) 065701. https://doi.org/10.1103/PhysRevE.84.065701.
[197] H.H. Huang et al., Int. J. Eng. Sci. 47 (4) (2009) 610–617. https://doi.org/10.1016/j.ijengsci.2008.12.007.
[198] F.M. Liu et al., Phys. Rev. B 94 (22) (2016) 224102. https://doi.org/10.1103/PhysRevB.94.224102.
[199] L. Quan, A. Alù, Phys. Rev. Lett. 123 (24) (2019) 244303. https://doi.org/10.1103/PhysRevLett.123.244303.
[200] L.R. Lu et al., Finite Elem. Anal. Des. 72 (2013) 1–12. https://doi.org/10.1016/j.finel.2013.04.005.
[201] J.J. Rong et al., Adv. Funct. Mater. 30 (50) (2020) 2005285. https://doi.org/10.1002/adfm.202005285.
[202] K. Donda et al., Smart Mater. Struct. 30 (8) (2021) 085003. https://doi.org/10.1088/1361-665X/ac0675.
[203] Y.F. Chen et al., J. Sound Vib. 544 (2023) 117410. https://doi.org/10.1016/j.jsv.2022.117410.
[204] Z.L. Du et al., Int. J. Mech. Sci. 255 (2023) 108441. https://doi.org/10.1016/j.ijmecsci.2023.108441.
[205] D. Li et al., J. Acoust. Soc. Am. 132 (4) (2012) 2823–2833. https://doi.org/10.1121/1.4744942.
[206] K.L. Manktelow et al., J. Mech. Phys. Solids 61 (12) (2013) 2433–2453. https://doi.org/10.1016/j.jmps.2013.07.009.
[207] H.W. Dong et al., J. Phys. D-Appl. Phys. 47 (15) (2014) 155301. https://doi.org/10.1088/0022-3727/47/15/155301.
[208] H.Y. Long et al., Phys. Rev. Appl. 18 (4) (2022) 044032. https://doi.org/10.1103/PhysRevApplied.18.044032.
[209] H.W. Dong et al., Struct. Multidiscip. Optim. 50 (4) (2014) 593–604. https://doi.org/10.1007/s00158-014-1070-6.
[210] H.W. Dong et al., Phys. Lett. A 378 (4) (2014) 434–441. https://doi.org/10.1016/j.physleta.2013.12.003.
[211] Y. Li et al., J. Sound Vib. 529 (2022) 116962. https://doi.org/10.1016/j.jsv.2022.116962.
[212] Y. Li et al., Int. J. Mech. Sci. 254 (2023) 108442. https://doi.org/10.1016/j.ijmecsci.2023.108442.
[213] H. Ronellenfitsch et al., Phys. Rev. Mater. 3 (9) (2019) 095201. https://doi.org/10.1103/PhysRevMaterials.3.095201.
[214] G.A. Gazonas et al., Int. J. Solids Struct. 43 (18–19) (2006) 5851–5866. https://doi.org/10.1016/j.ijsolstr.2005.12.002.
[215] S.L. Vatanabe et al., J. Acoust. Soc. Am. 136 (2) (2014) 494–501. https://doi.org/10.1121/1.4887456.
[216] S. Halkjær et al., Struct. Multidiscip. Optim. 32 (4) (2006) 263–275. https://doi.org/10.1007/s00158-006-0037-7.
[217] M. Wormser et al., Materials 10 (10) (2017) 1125. https://doi.org/10.3390/ma10101125.
[218] H.F. Chen et al., Struct. Multidiscip. Optim. 65 (9) (2022) 253. https://doi.org/10.1007/s00158-022-03355-1.
[219] S. Hedayatrasa et al., J. Mech. Phys. Solids 89 (2016) 31–58. https://doi.org/10.1016/j.jmps.2016.01.010.
[220] X.P. Zhang et al., Compos. Struct. 306 (2023) 116584. https://doi.org/10.1016/j.compstruct.2022.116584.
[221] S.J. Van Den Boom et al., Comput. Meth. Appl. Mech. Eng. 408 (2023) 115888. https://doi.org/10.1016/j.cma.2023.115888.
[222] Y.F. Chen et al., Comput. Struct. 182 (2017) 430–447. https://doi.org/10.1016/j.compstruc.2017.01.001.
[223] W.B. Li et al., Struct. Multidiscip. Optim. 60 (6) (2019) 2405–2415. https://doi.org/10.1007/s00158-019-02329-0.
[224] Z.X. Zhang et al., Comput. Mater. Sci. 139 (2017) 97–105. https://doi.org/10.1016/j.commatsci.2017.07.037.
[225] M. Li et al., Compos. Struct. 229 (2019) 111385. https://doi.org/10.1016/j.compstruct.2019.111385.
[226] F.L. Li et al., Int. J. Mech. Sci. 144 (2018) 110–117. https://doi.org/10.1016/j.ijmecsci.2018.05.042.
[227] X.P. Zhang et al., Comput. Mater. Sci. 160 (2019) 159–172. https://doi.org/10.1016/j.commatsci.2018.12.057.
[228] X.B. Miao et al., Eng. Optim. 55 (1) (2023) 125–139. https://doi.org/10.1080/0305215x.2021.1988587.
[229] P. Kudela et al., Mech. Syst. Signal Proc. 200 (2023) 110636. https://doi.org/10.1016/j.ymssp.2023.110636.
[230] X. Li et al., Comput. Meth. Appl. Mech. Eng. 361 (2020) 112737. https://doi.org/10.1016/j.cma.2019.112737.
[231] L.L. Wu et al., Extreme Mech. Lett. 36 (2020) 100657. https://doi.org/10.1016/j.eml.2020.100657.

Please cite this article in press as: H.-W. Dong et al., Materials Today, (2024), https://doi.org/10.1016/j.mattod.2024.09.012

[232] M. Aspelmeyer et al., Rev. Mod. Phys. 86 (4) (2014) 1391–1452. https://doi.org/10.1103/RevModPhys.86.1391.
[233] M. Forsch et al., Nat. Phys. 16 (1) (2020) 69–74. https://doi.org/10.1038/s41567-019-0673-7.
[234] S. Hong et al., Science 358 (6360) (2017) 203–206. https://doi.org/10.1126/science.aan7939.
[235] M. Metcalfe, Appl. Phys. Rev. 1 (3) (2014) 031105. https://doi.org/10.1063/1.4896029.
[236] F.L. Li et al., Wave Motion 50 (3) (2013) 525–541. https://doi.org/10.1016/j.wavemoti.2012.12.001.
[237] M.I. Hussein et al., J. Sound Vib. 307 (3–5) (2007) 865–893. https://doi.org/10.1016/j.jsv.2007.07.021.
[238] Z.X. Xu et al., Phys. Rev. Appl. 14 (5) (2020) 054016. https://doi.org/10.1103/PhysRevApplied.14.054016.
[239] M. Oddiraju et al., J. Mech. Des. 144 (2) (2022) 021707. https://doi.org/10.1115/1.4052300.
[240] K. Huang et al., IEEE Open J. Ultrason. Ferroelectr. Freq. Control 3 (2023) 166–175. https://doi.org/10.1109/OJUFFC.2023.3314396.
[241] J. Hyun et al., Appl. Phys. Lett. 115 (17) (2019) 173901. https://doi.org/10.1063/1.5111566.
[242] J. Hyun et al., Appl. Phys. Lett. 116 (23) (2020) 234102. https://doi.org/10.1063/5.0009799.
[243] Z. Liu et al., Struct. Health Monit. 22 (3) (2023) 1828–1843. https://doi.org/10.1177/14759217221114525.
[244] X.J. Zhang et al., Nat. Phys. 15 (6) (2019) 582-+. https://doi.org/10.1038/s41567-019-0472-1.
[245] X.Y. Zhuang et al., Mater. Des. 219 (2022) 110760. https://doi.org/10.1016/j.matdes.2022.110760.
[246] J.H. Zhang et al., Sci. China-Phys. Mech. Astron. 65 (5) (2022) 257011. https://doi.org/10.1007/s11433-021-1854-2.
[247] Y.F. Chen et al., Int. J. Mech. Sci. 260 (2023) 108669. https://doi.org/10.1016/j.ijmecsci.2023.108669.
[248] L.S. He et al., Mater. Des. 199 (2021) 109390. https://doi.org/10.1016/j.matdes.2020.109390.
[249] L. He et al., Sci. China-Phys. Mech. Astron. 65 (1) (2022) 214612. https://doi.org/10.1007/s11433-021-1787-x.
[250] J.C. Luo et al., Extreme Mech. Lett. 45 (2021) 101276. https://doi.org/10.1016/j.eml.2021.101276.
[251] J.C. Luo et al., J. Mech. Phys. Solids 176 (2023) 105325. https://doi.org/10.1016/j.jmps.2023.105325.
[252] Y.F. Chen et al., Adv. Theory Simul. 5 (6) (2022) 2200103. https://doi.org/10.1002/adts.202200103.
[253] Y. Lu, H.S. Park, Phys. Rev. B 103 (6) (2021) 064308. https://doi.org/10.1103/PhysRevB.103.064308.
[254] X.J. Zhang et al., Nature 618 (7966) (2023) 687–697. https://doi.org/10.1038/s41586-023-06163-9.
[255] X.W. Yang et al., J. Sound Vib. 383 (2016) 89–107. https://doi.org/10.1016/j.jsv.2016.07.022.
[256] Y. Noguchi et al., Int. J. Numer. Methods Eng. 113 (8) (2018) 1300–1339. https://doi.org/10.1002/nme.5616.
[257] R. Zhu et al., Phys. Rev. B 86 (14) (2012) 144307. https://doi.org/10.1103/PhysRevB.86.144307.
[258] H.W. Dong et al., Sci. Rep. 8 (2018) 2247. https://doi.org/10.1038/s41598-018-20579-8.
[259] J.Y. Zhang et al., Extreme Mech. Lett. 48 (2021) 101372. https://doi.org/10.1016/j.eml.2021.101372.
[260] Y. Noguchi et al., Comput. Meth. Appl. Mech. Eng. 335 (2018) 419–471. https://doi.org/10.1016/j.cma.2018.02.031.
[261] V.M. García-Chocano et al., Appl. Phys. Lett. 99 (7) (2011) 074102. https://doi.org/10.1063/1.3623761.
[262] Y. Noguchi et al., Adv. Eng. Mater. 25 (4) (2023) 2201104. https://doi.org/10.1002/adem.202201104.
[263] J. Chen et al., Extreme Mech. Lett. 55 (2022) 101827. https://doi.org/10.1016/j.eml.2022.101827.
[264] Z. Liu et al., Compos. Struct. 295 (2022) 115863. https://doi.org/10.1016/j.compstruct.2022.115863.
[265] Y.-T. Luo et al., Research 2020 (2020) 8757403. https://doi.org/10.34133/2020/8757403.
[266] Z.-W. Wang et al., Sci. China-Phys. Mech. Astron. 66 (2) (2023) 224311. https://doi.org/10.1007/s11433-022-1984-1.
[267] B. Ahn et al., Comput. Meth. Appl. Mech. Eng. 333 (2018) 176–196. https://doi.org/10.1016/j.cma.2018.01.016.
[268] C.G. Méndez et al., Int. J. Numer. Methods Eng. 112 (10) (2017) 1353–1380. https://doi.org/10.1002/nme.5560.
[269] J.M. Podestá et al., J. Mech. Phys. Solids 128 (2019) 54–78. https://doi.org/10.1016/j.jmps.2019.03.018.
[270] R. Yera et al., Appl. Mater. Today 18 (2020) 100456. https://doi.org/10.1016/j.apmt.2019.100456.
[271] X. Yang, Y.Y. Kim, Compos. Struct. 201 (2018) 161–177. https://doi.org/10.1016/j.compstruct.2018.06.022.
[272] A. Bossart, R. Fleury, Phys. Rev. Lett. 130 (20) (2023) 207201. https://doi.org/10.1103/PhysRevLett.130.207201.
[273] H. Goh, A. Alù, Phys. Rev. Lett. 128 (7) (2022) 073201. https://doi.org/10.1103/PhysRevLett.128.073201.
[274] N.F. Yu et al., Science 334 (6054) (2011) 333–337. https://doi.org/10.1126/science.1210713.
[275] B. Ahn et al., Comput. Meth. Appl. Mech. Eng. 357 (2019) 112582. https://doi.org/10.1016/j.cma.2019.112582.
[276] L.J. Fan, J. Mei, Phys. Rev. Appl. 14 (4) (2020) 044003. https://doi.org/10.1103/PhysRevApplied.14.044003.
[277] J. Mei et al., Phys. Rev. Appl. 18 (1) (2022) 014002. https://doi.org/10.1103/PhysRevApplied.18.014002.
[278] H. Ding et al., Phys. Rev. Appl. 16 (6) (2021) 064035. https://doi.org/10.1103/PhysRevApplied.16.064035.
[279] J.W. Guo et al., J. Sound Vib. 520 (2022) 116631. https://doi.org/10.1016/j.jsv.2021.116631.
[280] H.T. Zhou et al., Mech. Syst. Signal Proc. 177 (2022) 109228. https://doi.org/10.1016/j.ymssp.2022.109228.
[281] Y. Noguchi et al., Appl. Phys. Lett. 107 (22) (2015) 221909. https://doi.org/10.1063/1.4936997.
[282] S.W. Fan et al., Appl. Phys. Lett. 123 (10) (2023) 102202. https://doi.org/10.1063/5.0154688.
[283] X.D. He et al., J. Mech. Phys. Solids 174 (30) (2023) 105247. https://doi.org/10.1016/j.jmps.2023.105247.
[284] H.T. Zhou et al., Adv. Sci. 10 (19) (2023) 2207181. https://doi.org/10.1002/advs.202207181.
[285] K. Melde et al., Sci. Adv. 9 (6) (2023) eadf6182. https://doi.org/10.1126/sciadv.adf6182.
[286] J.J. Rong, W.J. Ye, Acta Mater. 185 (2020) 382–399. https://doi.org/10.1016/j.actamat.2019.12.017.
[287] Z. Liu et al., Ultrasonics 139 (13) (2024) 107295. https://doi.org/10.1016/j.ultras.2024.107295.
[288] Z.L. Zhou et al., Natl. Sci. Rev. 9 (8) (2022) nwab171. https://doi.org/10.1093/nsr/nwab171.
[289] R. Ichige et al., Sensors and Actuators a-Physical 318 (2021) 112488. https://doi.org/10.1016/j.sna.2020.112488.
[290] S. Shan et al., Smart Mater. Struct. 26 (2) (2017) 025019. https://doi.org/10.1088/1361-665x/26/2/025019.
[291] S. Shan et al., Smart Mater. Struct. 27 (10) (2018) 105006. https://doi.org/10.1088/1361-665X/aad938.
[292] Z. Liu et al., Smart Mater. Struct. 31 (6) (2022) 065001. https://doi.org/10.1088/1361-665X/ac64db.
[293] C. Scheibner et al., Nat. Phys. 16 (4) (2020) 475–480. https://doi.org/10.1038/s41567-020-0795-y.
[294] Z.X. Chen et al., Sci. Adv. 7 (45) (2021) eabj1198. https://doi.org/10.1126/sciadv.abj1198.
[295] M.P. Zaletel et al., Rev. Mod. Phys. 95 (3) (2023) 031001. https://doi.org/10.1103/RevModPhys.95.031001.
[296] J. Zhang et al., Nature 543 (7644) (2017) 217–220. https://doi.org/10.1038/nature21413.
[297] C.K. Liu et al., Phys. Rev. Lett. 127 (8) (2021) 084301. https://doi.org/10.1103/PhysRevLett.127.084301.
[298] C. Zhang et al., ACS Appl. Mater. Interfaces 11 (18) (2019) 17050–17055. https://doi.org/10.1021/acsami.9b02490.
[299] X.W. Li et al., Small 17 (24) (2021) 2100336. https://doi.org/10.1002/smll.202100336.
[300] X.W. Li et al., Adv. Mater. 33 (44) (2021) 2104552. https://doi.org/10.1002/adma.202104552.
[301] G. Feng et al., Appl. Surf. Sci. 463 (2019) 741–746. https://doi.org/10.1016/j.apsusc.2018.09.005.

Please cite this article in press as: H.-W. Dong et al., Materials Today, (2024), https://doi.org/10.1016/j.mattod.2024.09.012

[302] Z.D. Li et al., Appl. Phys. Lett. 118 (16) (2021) 161903. https://doi.org/10.1063/5.0044656.
[303] H. Cui et al., Science 376 (6599) (2022) 1287–1293. https://doi.org/10.1126/science.abn0090.
[304] J.J. Slim et al., Nature 627 (8005) (2024) 767–771. https://doi.org/10.1038/s41586-024-07174-w.
[305] J.W. Guo et al., J. Acoust. Soc. Am. 149 (1) (2021) 70–81. https://doi.org/10.1121/10.0002990.
[306] X.Q. Ma, Z.T. Su, Sci. China-Technol. Sci. 63 (12) (2020) 2491–2504. https://doi.org/10.1007/s11431-019-1501-3.
[307] C. Rasmussen, A. Alù, Proc. Natl. Acad. Sci. U. S. A. 118 (30) (2021) e2024984118. https://doi.org/10.1073/pnas.2024984118.
[308] K. Liu et al., Science 377 (6609) (2022) 975–981. https://doi.org/10.1126/science.abn1459.
[309] C. Qian et al., Light Sci. Appl. 9 (3) (2020) 2095. https://doi.org/10.1038/s41377-020-0303-2.
[310] C. Liu et al., Nature Electron. 5 (2) (2022) 113–122. https://doi.org/10.1038/s41928-022-00719-9.

Please cite this article in press as: H.-W. Dong et al., Materials Today, (2024), https://doi.org/10.1016/j.mattod.2024.09.012